Available online at www.sciencedirect.com

SCIENCE DIRECT®

ELSEVIER

Coordination Chemistry Reviews 249 (2005) 799–827

COORDINATION CHEMISTRY REVIEWS

www.elsevier.com/locate/ccr

Review

Structural chemistry of complexes of $(n-1)d^{10}\ ns^m$ metal ions with β-N-donor substituted thiolate ligands ($m = 0, 2$)

Holger Fleischer*

Institut für Anorganische Chemie und Analytische Chemie, Johannes Gutenberg Universität Mainz, Duesbergweg 10–14, D-55099 Mainz, Germany

Contents

Abbreviations: CM(M), co-ordination mode of metal M; e.s.d., estimated standard deviation; *fac*, facial configuration of octahedral complexes with M(N3S3) co-ordination mode; HSR, general thiol, R being an alkyl or aryl type; L, general N,S-ligand; lp, lone pair of electrons; M, general metal; *mer*, meridional configuration of octahedral complexes with $M(N_3S_3)$ co-ordination mode; $N_xS_yX_z$-ligand, A $(x+y+z)$ dentate ligand with x N-, y S- and z X-donor atoms; pbp, pentagonal bipyramidal co-ordination geometry; phen, 1,10-phenanthroline; sp/ψ-sp, square pyramidal/pseudo square pyramidal co-ordination geometry; tbp/ψ-tbp, trigonal biypramidal/pseudo trigonal bipyramidal co-ordination geometry

* Tel.: +49 6131 392 5886; fax: +49 6131 392 5336.
E-mail address: fleische@uni-mainz.de.

doi:10.1016/j.ccr.2004.08.024

Abstract

The molecular structures of several d^{10} metal ion complexes with 2-amino or 2-imino substituted thiolate ligands, derived from 2-aminoethanethiol, 2-(mercaptomethyl)pyridine, 2-aminobenzenethiole, and 8-mercaptoquinoline, are presented. Since ligand field stabilization energy is absent, the complexes display a large variety of co-ordination numbers and geometries around the metal centers. Distortions from ideal tetrahedral or trigonal bipyramidal configurations are discussed in terms of special structural parameters. In contrast to thiolate ligands that lack additional donor atoms and thus form oligo- or poly-nuclear complexes, the β-N donor group stabilizes mono-nuclear complexes in many cases. In that respect, the number of donor atoms available per metal centre is decisive. Due to its importance for biological systems as compared to the other elements dealt with in this review, there are many more structurally characterized complexes with N,S-donor ligands for Zn^{2+} than for any other d^{10} ion. Significant structural differences concerning co-ordination number and structural parameters occur between Zn^{2+} on one hand and Cd^{2+}/Hg^{2+} complexes on the other. With tetraco-ordinate d^{10} s^2 ions pseudo trigonal bipyramidal structures occur as well as pseudo square pyramidal structures.

Keywords: Thiolate ligands; Structural chemistry; d^{10} metal ions

1. Introduction

1.1. Scope

This review deals with the molecular and crystal structures of complexes of closed d-shell group 11–15 metal ions with β-N-donor thiolate ligands, where the nitrogen atom is of an amine, imine or amide type. The survey of the literature and of the crystal structures deposited in the Cambridge Crystallographic Database covered material up to 2003. In the course of the present paper, the title ligands are referred to as N,S-ligands and the scope of this review is limited to them. N-donor substituted thioethers, thiocarbamates, or thiones which also frequently occur as N,S-ligands are not dealt with, neither are N-donor thiolate ligands with the N-atom not being in the β-position. On the other hand, the N,S-ligands presented herein often contain additional N, O or S-donor atoms. From a biological view, Zn^{2+} is certainly the most important of the d^{10} metal ions in these complexes, since N,S-ligands can mimic naturally occurring ligands like cysteine and cysteamine. Considering the co-ordination properties of thiolates, RS^-, and amines, NR_3, in terms of the HSAB principle, amino substituted thiolates prefer binding to soft metal ions, e.g. Ag^+, Hg^{2+}, Zn^{2+}, Pb^{2+} and Sn^{2+}. Also, importantly, d^{10} ions do not derive ligand field stabilization energy benefits by assuming certain co-ordination numbers or geometries. Shape, size and topology of the complexes will hence depend mainly on the steric requirements of the ligands and may show gradual changes between different compounds. Therefore, it was of interest to compare the structural chemistry of the Zn^{2+} complexes to those of these d^{10} metal ions that may compete with the Zn^{2+} for binding to N,S-donor sites in peptides and proteins.

1.2. Earlier reviews on related subjects

Several reviews dealing with aspects of thiolate ligands were published in recent years. Nearly 20 years ago Dance gave a comprehensive overview on the structural chemistry of metal thiolate complexes [1]. Krebs et al. reported on thiolate clusters and their importance in bioinorganic chemistry [2], while Dilworth and co-workers focused on transition metal thiolate complexes [3,4]. Several reviews dealing with special aspects of thiolate ligands containing N-donor sites have been published. In 1974, Ali and Livingstone reported on metal complexes of sulphur-nitrogen chelating agents, but little structural information is given in there [5]. Brooker gave an overview on complexes of thiophenolate-containing Schiff-base macrocycles and their amine analogues [6], Raper published several reviews on complexes of heterocyclic thiones [7–9], and Garcia-Vazquez et al. presented methods for the electrochemical synthesis of metal complexes of N,S-donor ligands [10]. Review articles on closely related areas were given by Danks et al. on the chemistry of mixed nitrogen- and sulfur-donor tridentate macrocycles [11], Dilworth and Wheatley on the co-ordination chemistry of phosphorus sulfur donor ligands [12], Casas et al. on the structural chemistry of main group metal complexes of semicarbazones and thiosemicarbazones [13], and Pellerito and Nagy on organotin(IV) complexes formed with biologically active ligands [14].

The increasing interest in thiolate complexes in general has ensued as a result of a diversity of factors:

1. Thiolate complexes are of great importance from a bioinorganic point of view, mainly due to the presence of thiolate donors in the co-ordination sphere of many metal ions in very diverse metalloproteins (see, e.g. [2]).
2. The growth in the utilization of certain thiolates, e.g. in medical chelation therapy and for the treatment of special diseases like cystinosis [15–17].
3. The use of volatile molecular thiolates as starting materials for chemical surface deposition of layers of metals or sulfides from vapor phase, (CVD). This requires the presence of low molecular weight species that are easily volatilized, at least to low pressure and that are thermally stable to sublime without decomposition [18–20].

Since the number of structurally investigated d^{10} metal ion complexes with N,S-donor ligands has substantially increased over the recent years, this work gives a comprehensive and comparative review of the title subject.

1.3. Organization of the material

First, the ligands that occur within this review are presented, together with references to the syntheses for most of them. The section dealing with the structural chemistry of the metal complexes is subdivided into five subsections, each dealing with a single group of the elements from 11 to 15. Within each subsection, important structural parameters describing the co-ordination of the metal ions/atoms and pictures of selected molecular structures are presented. The complexes are briefly and comparatively described, the emphasis being on co-ordination modes and geometries. For $(n-1)\ d^{10}\ ns^2$ configured metal ions, the stereochemical role of the lone pair will be analyzed. Trends of parameters for different complexes will be outlined and differences occurring for a given metal ion with different ligands will be identified.

All interatomic distances are given in Å, and all bond angles in degree (°). If the e.s.d.s are readily available, their values are given in the usual manner. Atoms are presented as spheres in pictures of molecular structures, i.e. non-isotropic displacements are not displayed. Bonds considered to be covalent are represented by full lines, while co-ordinative or bridging bonds as well as intermolecular contacts are depicted as broken lines.

2. Syntheses of ligands and metal thiolates

2.1. Syntheses of ligands

The ligands presented in Schemes 1–3 are those referred to at some stage within this review. Scheme 1 comprises the bidentate, Scheme 2 the terdentate and Scheme 3 the tetra- and higher dentate ligands. Since most of the ligands have structures that are not easy to represent in a molecular formula, abbreviations were devised for them. For a more systematic approach, the general abbreviation "L" for "ligand" is used throughout the paper which is given a superscript in order to distinguish between them. Ligands that do not significantly differ from each other share the same number and lower case letters are added for distinction. Depending on the number of protons that can be replaced by metal ions, the free ligands are denoted as HL, H_2L, H_3L, etc. The superscript of the ligand increases with the number of donor atoms, i.e. the order is bidentate ligands (HL^{1a}–HL^{8m}), tridentate ligands (HL^{9a}–H_2L^{19}), and tetra- and higher dentate ligands (HL^{20}–$H_{10}L^{28}$). For each set, the superscript increases first with the number of mercapto groups and then with the number of hydroxy groups. Within a subset of ligands having the same number of mercapto/hydroxy groups, the numbering increases in the sequence (aliphatic thiol + aliphatic amine) < (aliphatic thiol + aromatic amine) < (aromatic thiol + aromatic amine). The remaining order was achieved by having lower numbers for the more simple ligands which maybe somewhat arbitrary in special cases.

Some of the ligands presented here can be purchased as such or in the hydrochloride form from chemical suppliers. In these cases, no special notes are given to their synthesis. As well, no special references are given to ligands that were formed in situ by redox reaction with metal ions or oxygen. However, elaborate synthetic procedures are necessary for several ligands, and in these cases, the references are given in the footnotes of those schemes where the ligands are presented. A lot of these syntheses are variations of the general procedures of Reynolds et al. (mercaptoethylation of amines with ethylene sulfide) [21], and Harley-Mason (alkaline cleavage of thiourionium salts) [22], by which the mercapto group is incorporated in the molecule.

Of all the above-mentioned ligands, 8-mercaptoquinoline and its derivatives (HL^{8a}–HL^{8m}) are those most often found in the complexes presented here. It is quite surprising that of the rather simple ligands HL^{1a}, HL^{1c} and HL^{6} little structural complex chemistry is known with d^{10} ions.

2.2. Syntheses of metal thiolates

Several approaches can be used for the preparation of the metal thiolate complexes, enabling the synthetic chemist to choose the most appropriate for the target compound. Some of the general strategies will be presented here and then referred to in Section 3.

2.2.1. Salt metathesis

This is certainly the most common synthetic route toward metal thiolates. Either the thiol itself is used, together with a base (B) to scavenge the hydrogen halide, or sodium thiolate:

$$MX_n + n\text{HSR} + n\text{B} \rightarrow M(SR)_n + n[\text{HB}]X \qquad (1)$$

$$MX_n + n\text{NaSR} \rightarrow M(SR)_n + n\text{NaX} \qquad (2)$$

X maybe a halide or a weakly co-ordinating anion like BF_4^- or ClO_4^-.

2.2.2. Protolysis of M–O, M–N or M–C bonds

If the sum of energies of the M–S and X–H bonds (X = O, N, S) exceeds that of the M–X and S–H bonds, the metal thiolate is accessible via simple metathesis reactions. A few examples are given in the following equations:

$$MO_{n/2} + n\text{HSR} \rightarrow M(SR)_n + (n/2)H_2O \qquad (3)$$

$$M(OR')_n + n\text{HSR} \rightarrow M(SR)_n + n\text{HOR}' \qquad (4)$$

$$M[N(SiMe_3)_2]_n + n\text{HSR} \rightarrow M(SR)_n + n\text{HN}(SiMe_3)_2 \qquad (5)$$

$$MR'_n + n\text{HSR} \rightarrow M(SR)_n + n\text{RH} \qquad (6)$$

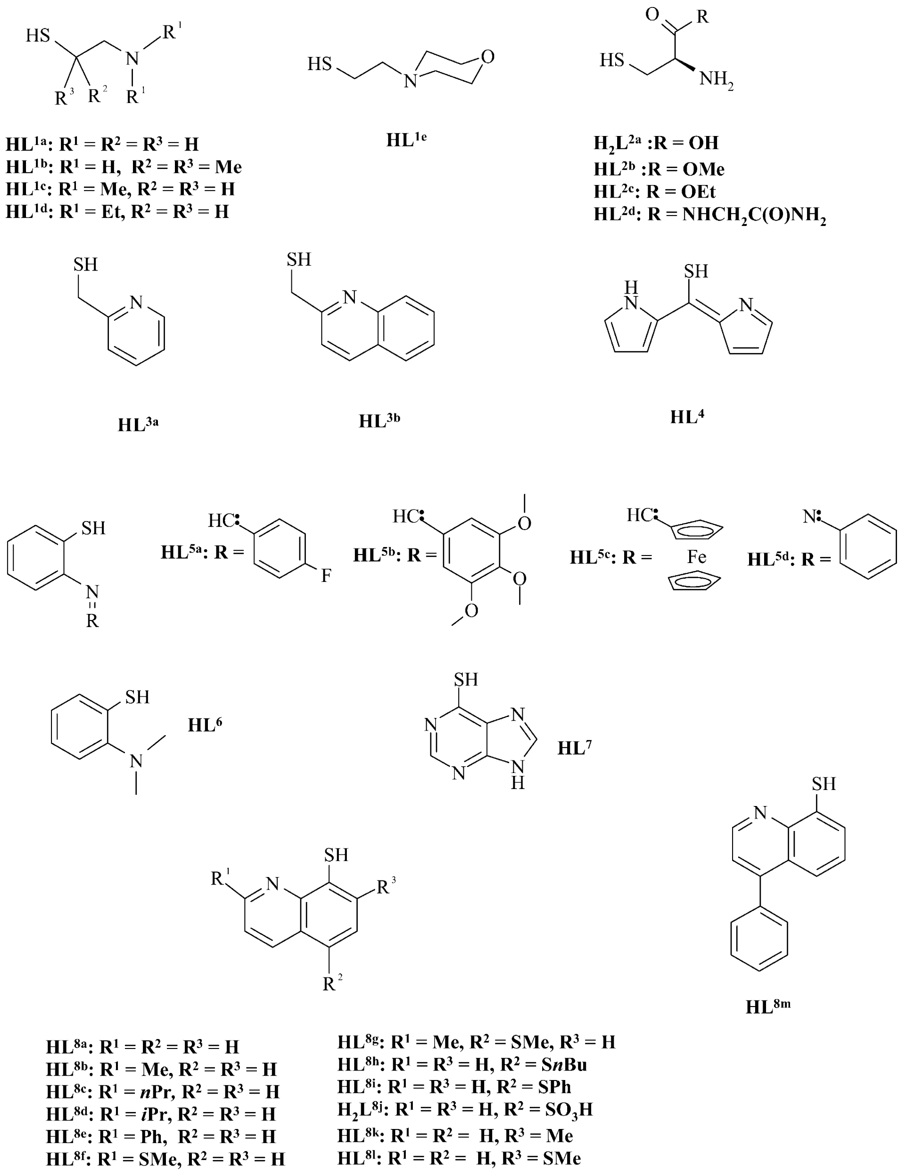

Scheme 1. Bidentate ligands. References to syntheses of the ligands: HL^{1b} [23]; HL^{1d} [24]; HL^{1e} [25]; HL^{2d} [26]; HL^{3a} and HL^{3b} [27]; HL^{4} [28,29]; HL^{5a} [30]; HL^{5b} [31]; HL^{5c} [32]; HL^{5d} [33]; HL^{8b} [34]; HL^{8c} [35]; HL^{8d} [36]; HL^{8e} [37]; HL^{8f} [38];HL^{8g} [39]; HL^{8h} [39]; HL^{8i} [40]; HL^{8j} [41]; HL^{8k} [42]; HL^{8l} [43]; HL^{8m} [44].

These reactions are especially feasible for thiolates of group 12 elements, in the case of X = N or C also for group 13 and 14 elements. The advantage over the salt metathesis is the facile separation of the more or less volatile side products from the metal thiolates.

2.2.3. Electrochemical synthesis

Electrochemical synthesis of $M(SR)_n$ work via anodic oxidation of the M to the corresponding cation (M^{n+}) in a solution containing the required thiolate (RS^-) or by cathodic reduction of a symmetric disulphide (RSSR) to its corresponding thiolate (RS^-) in a solution of the respective metal ion (M^{n+}). Of course, both syntheses can be combined in a single electrochemical cell to yield $M(SR)_n$ from M and RSSR [10,73].

3. Structures of metal complexes

3.1. Group 11 complexes

Copper(I) arene thiolates are well known in the literature and generally have multi-nuclear, oligomeric or polymeric structures [74–76]. Cu^I-thiolate complexes with N,S-ligands are of interest due to their biomimetic potential toward the enzyme cytochrome-*c*-oxidase. This enzyme contains the homodimetallic mixed valence CuA centre, the copper atoms of which are co-ordinated by two bridging cysteine groups and one additional histidine residue [63].

1 is part of a thiolate-bridged, fully delocalized mixed-valence dicopper (I,II) complex that models the Cu_A biological electron transfer site. The two equivalent copper centers

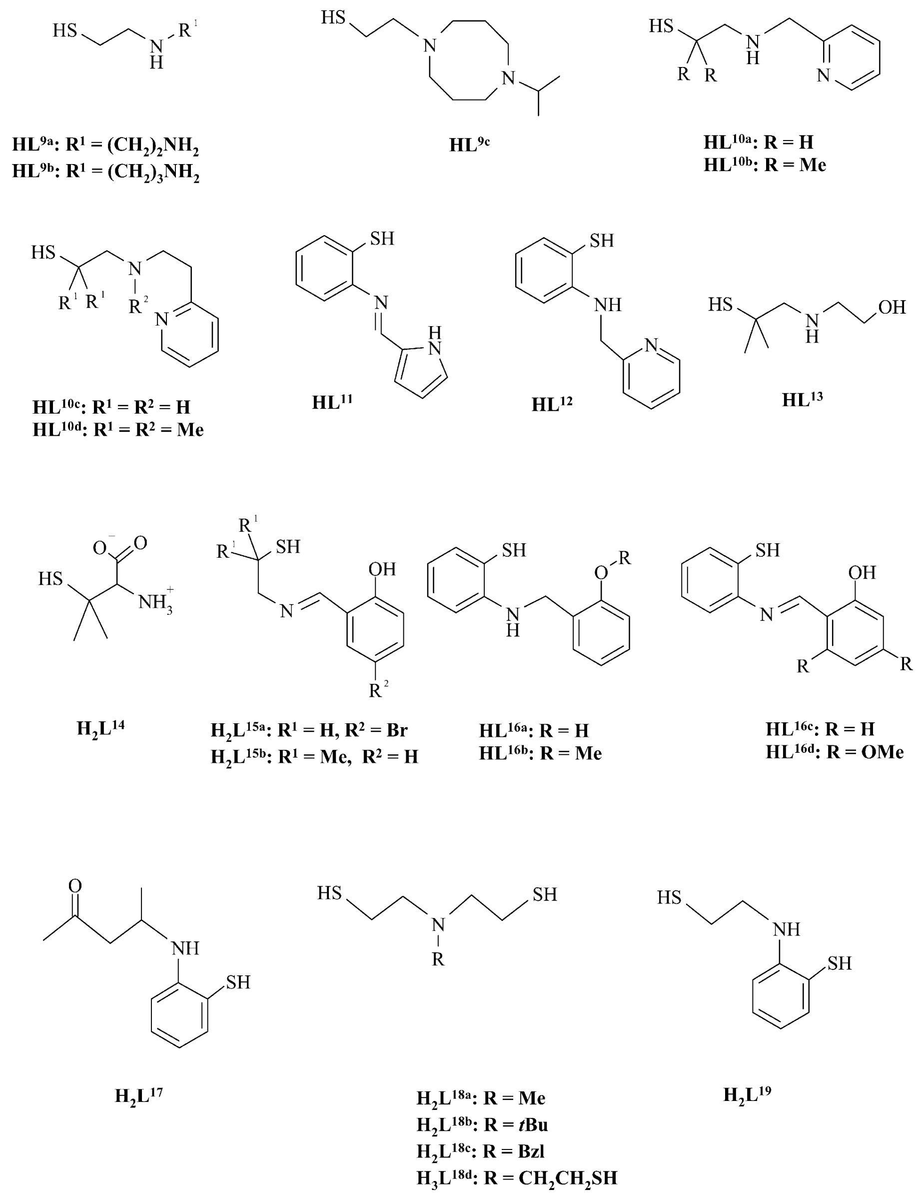

Scheme 2. Terdentate ligands. References to syntheses of the ligands: HL^{9a} and HL^{9b} [45]; HL^{9c} [46]; HL^{10a} and HL^{10c} [45]; HL^{10b} [47]; HL^{10d} [48]; HL^{11} [49]; HL^{12} [50]; HL^{13} [51]; H_2L^{15a} [52]; H_2L^{15b} [51]; HL^{16a} [53]; HL^{16b} [54]; HL^{16c} [55]; HL^{16d} [56]; H_2L^{17} [57]; H_2L^{18a} [22]; H_2L^{18b} [22]; H_2L^{18c} [25]; H_3L^{18d} [22]; H_2L^{19} [58].

are related by inversion symmetry and connected via two thiolate bridges forming a Cu_2S_2-ring (see Fig. 1). The geometry of each of the metal ions is best described as distorted trigonal pyramidal with the S(1), S(1a), and N(1) defining the trigonal plane from which the Cu ion is only slightly displaced (on average 0.20 Å for the two independent dimers) towards N(2).

2 displays a $Cu(NS_2)$ co-ordination mode for Cu^I with a trigonal planar geometry. The trimer comprises a six-membered Cu_3S_3-ring with a distorted chair conformation (a(Cu–S–Cu) = 75.2(1)°, a(S–Cu–S) = 141.6(1)° in which the N atoms occupy approximately the axial positions of the Cu atoms. Changing the ligand from L^6 to 8-dimethylamino-1-naphthalinethiolate (a γ-N substituted thiolate ligand) resulted in a three-layered nonamer, displaying tetra- and two co-ordinated Cu^I atoms [77].

3a and **3b** display eight-membered Cu_4S_4 rings as central structural units of their molecules (see Fig. 1) [63]. The copper ions are arranged in a planar rhomboidal fashion with close Cu···Cu distances (2.647(1)–2.705(1) Å), the S atoms laying above and below the plane. The structure is thus of a distorted As_4S_4-type, the Cu atoms occupying the sites of the S atoms and the S atom the sites of the As atoms. Both **3a** and **3b** exhibit two sorts of differently co-ordinated Cu^I ions: Cu(1) and Cu(3) are distorted tetrahedrally co-ordinated by two S and two N atoms while Cu(2) and Cu(4) bind to two S atoms only. A similar structural motif is found in the Ag_4S_4 ring of compound **5** in which

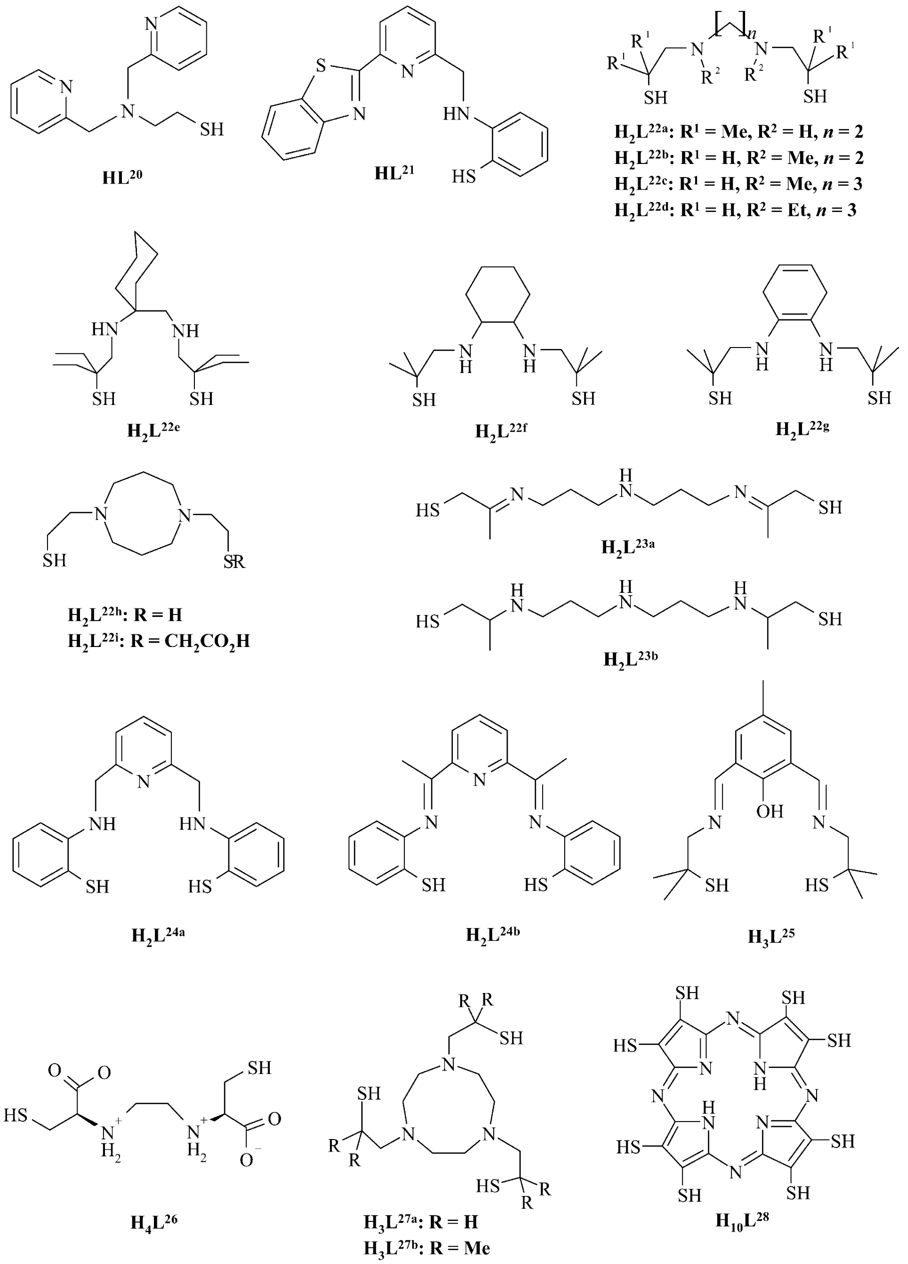

Scheme 3. Tetra- and higher dentate ligands. References to syntheses of the ligands: HL^{20} [59]; H_2L^{22a} [60]; H_2L^{22b} [21,61]; H_2L^{22c} and H_2L^{22d} [62,63]; H_2L^{22e} [64,65]; H_2L^{24a} [66]; H_2L^{24b} [67]; H_3L^{25} [68]; H_4L^{26} [69]; H_3L^{27a} [70]; H_3L^{27b} [71]; $H_{10}L^{28}$ [72].

the Ag ions display $Ag(N_2S_2)$ and $Ag(S_2)$ co-ordination modes.

4 exhibits a rather complicated structure which is best described as a polymer of penta-nuclear $[Ag(L^{1c})]_5$ units (see Fig. 1). Of the five L^{1c} ligands, only two co-ordinate in a bidentate N,S-mode. Ag–S distances and S–Ag–S angles vary over a wide range and there are three different co-ordination modes for the Ag atoms. Ag(3) is nearly linearly co-ordinated by two S atoms and also shows three short Ag · · · Ag contacts (2.873(1)–2.998(1) Å) to the other Ag atoms within the penta-nuclear unit. Ag(4) and Ag(5) display virtually planar $Ag(S_3)$ co-ordination modes, the sum of the three *a*(S–Ag–S) at each Ag being 359.7 and 359.8°, respectively. Finally Ag(1) and Ag(2) exhibit a $Ag(NS_3)$ co-ordination mode with a distorted tetrahedral geometry.

6 contains two differently co-ordinate Au^I atoms, since L^{8a} acts in a bidentate fashion towards Au(1) and in a monodentate mode towards Au(2). Interestingly, Au(2) displays a larger Au–S distance than Au(1), in spite of its lower co-ordination number. The S atom bridges Au(1) and Au(2) which exhibit a close distance to each other (3.264 and 3.370 Å). Such Au · · · Au contacts were found in many other Au^I-complexes [78]. Distances of the P atoms to the two differently co-ordinated Au^I ions are nearly equal (2.264–2.272 Å; Table 1).

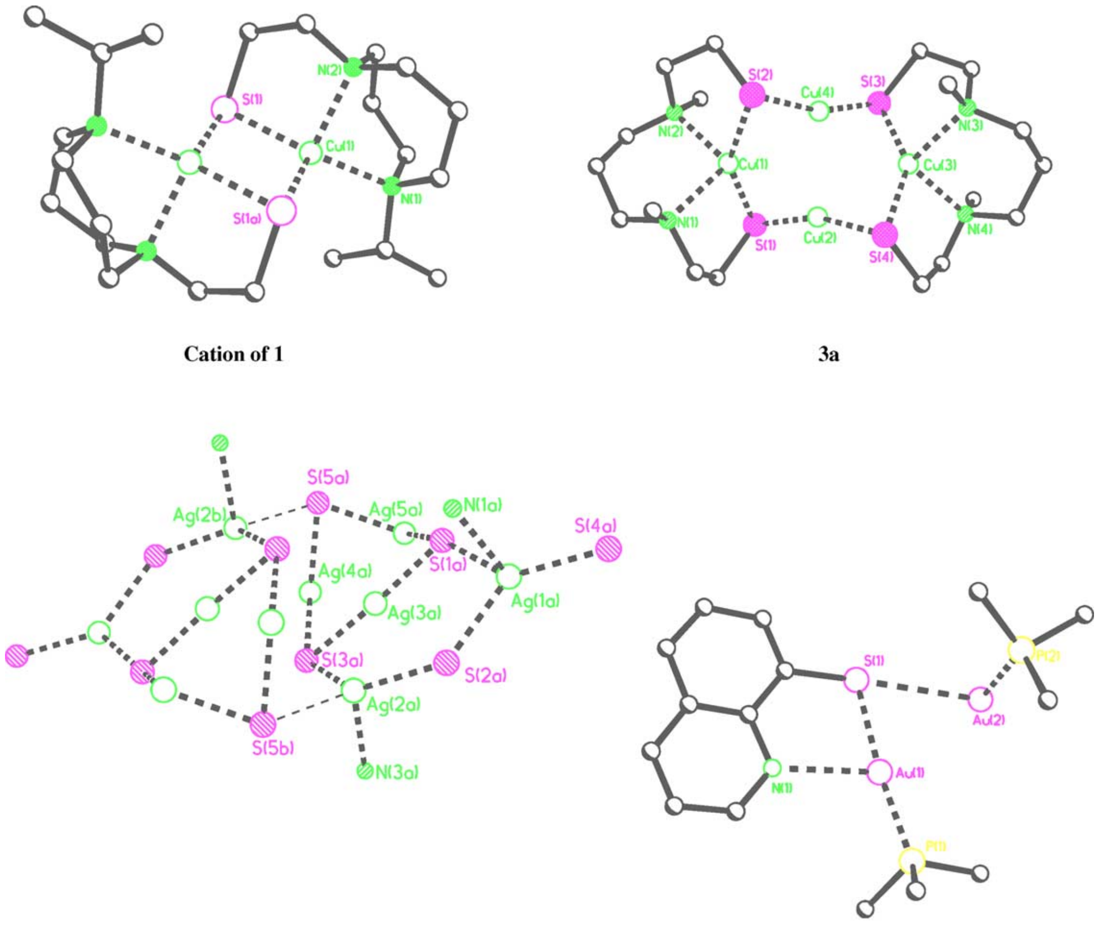

Cation of 1

3a

4

6

Fig. 1. Molecular structures of selected group 11 complexes. All H atoms are omitted for clarity. In **4**, all C atoms are omitted and the interaction between the penta-nuclear units in the solid state is depicted by dotted lines. In **6**, all C atoms of the phenyl groups are omitted except for the ipso C atoms.

3.2. *Group 12 complexes*

The Zn^{2+} ion is known to have a high affinity for nitrogen and sulfur donor ligands, as demonstrated by a considerable body of knowledge on Zn(N,S ligand) complexes [81]. The purpose of the investigations into these Zn-complexes is twofold: Firstly, one wants to gain an understanding of the factors controlling the co-ordination behavior (stoichiometries, co-ordination numbers, thiolate bridging, stabilities, etc.). The second aim is to learn how to construct structural

Table 1
Selected structural parameters for Cu^I-, Ag^I- and Au^I-complexes

Compound	CM(M)	*d*(M–S)	*d*(M–N)	*a*(S–M–S)	*a*(N–M–N)	References
$[Cu_2(L^{9c})_2](SO_3CF_3)$, **1**	$Cu(N_2S_2)$	2.250(1)/2.292(1)	2.115(3)/2.125(3)	99.6(1)	87.2(1)	[46]
$[Cu(L^6)]_3$, **2**	$Cu(NS_2)$	2.198(1)/2.222(1)	2.170(4)	141.6(1)		[77]
$[Cu_4(L^{22c})_2]$, **3a**	$Cu(N_2S_2)$	2.262(2)–2.271(2)	2.186(4)–2.220(4)	146.7(1)/144.8(1)	96.9(1)/95.5(1)	[63]
	$Cu(S_2)$	2.157(2)–2.173(2)		162.7(1)		
$[Cu_4(L^{22d})_2]$, **3b**	$Cu(N_2S_2)$	2.273(1)	2.196(2)	149.1(1)	97.9(1)	[63]
	$Cu(S_2)$	2.172(1)		157.8(1)		
$[Ag(L^{1c})]_5{\cdot}0.5H_2O$, **4**	$Ag(NS_3)$	2.468(2)–2.667(2)	2.482(6)/2.498(6)	91.3(1)–139.9(1)		[79]
	$Ag(S_3)$	2.478(2)–2.623(2)		101.1(1)–131.8(1)		
	$Ag(S_2)$	2.395(2)/2.408(2)		174.9(8)		
$[Ag(L^{8e})]_4$, **5**	$Ag(N_2S_2)$	2.430/2.455	2.533/2.598	154.0	83.4	[37]
	$Ag(S_2)$	2.381		176.0		
$[Au_2(L^{8a})(PPh_3)_2]BF_4$, **6**[a]	Au(AuNPS)	2.359/2.368	2.865/2.590			[80]
	Au(SAuP)	3.176/3.476				

[a] Structure contains two crystallographically different $[Au_2(L^{8a})(PPh_3)_2]BF_4$ units.

and possibly functional models of enzymes containing zinc in a $Zn(N_xY_y)$ environment [50]. In the zinc finger proteins [82], the so called “structural” zinc is almost always attached to at least one sulfur atom of cysteine, as is the “functional” zinc in the active centers of the enzymes liver alcohol dehydrogenase [83], spinach carbonic anhydrase [84], or bovine aminolaevulinate dehydratase [85]. In these enzymes, the Zn^{2+} ion is surrounded by a N_xS_y donor set provided by the amino acids histidine and cysteine. According to Brand and Vahrenkamp [86], the modelling of such a ZnN_xS_y environment requires multidentate ligands which ideally should fulfill the following conditions: (i) they should contain the correct number of N and S donors, (ii) they should encapsulate the metal such that oligomerization via bridging sulfur atoms are prevented, (iii) they should leave room for a labile ligand which may be replaced by a reacting substrate, and (iv) they should provide the right charge and electronic environment for the metal to tune it for its catalytic function.

It is not surprising therefore, that there are much more structurally characterized complexes with N,S-donor ligands for Zn^{2+} than for any other d^{10} ion due to the greater biological importance compared with other elements discussed in this review.

3.2.1. *Complexes of Zn^{II}*

Among many others, Vahrenkamp and co-workers have contributed a substantial body of information about the structures of Zn^{2+} complexes with N,S-ligands. As well a lot of N,S-ligand syntheses are due to the efforts of these groups.

3.2.1.1. Mono-nuclear Zn^{II} complexes displaying $Zn(N_2S_2)$ co-ordination mode. The simplest complexes of this type are built up of one Zn^{2+} ion and two identical, bidentate N,S-chelating ligands derived from 2-aminoethanethiol (HL^{1a}, aliphatic thiol with aliphatic amine), 2-pyridylmethanethiol (HL^{3a}, aliphatic thiol with aromatic amine), and 2-aminobenzenethiol (HL^{6a}, aromatic thiol with aromatic amine). Such a co-ordination mode is found in complexes **7–13**. As well, a single tetradentate N_2S_2-ligand is feasible, as in complexes **15a** and **15b**. Another type of $Zn(N_2S_2)$ co-ordination mode is realized in complex **14**. Here, Zn^{2+} binds to two N_2S-ligands, one of which acts in a mono and the other in a terdentate binding mode. Examples are depicted in Fig. 2. In all cases Zn^{2+} displays a more or less distorted tetrahedral environment in which the S–Zn–S angle is wider than the N–Zn–N angle (see Fig. 2 and Table 2). The parameter $a(ZnN_2S_2)$ describes the dihedral angle between the ZnS_2 and the ZnN_2 plane for a $Zn(N_2S_2)$ co-ordination. It is 90.0° for an ideal tetrahedral and 0.0° for a planar configuration. With the exception of **11c**, for which the angle between the ZnS_2 and the ZnN_2 plane is rather small, $a(ZnN_2S_2)$ lies between about 60 and 80° in all other cases, i.e. much closer to a tetrahedral than a square planar arrangement. Zn–S distances vary over a range of about 0.10 Å, without significant difference between aliphatic and aromatic thiolate ligands. The majority of the distances lie between 2.25 and 2.28 Å, hence d(Zn–S) does not vary much for the $Zn(N_2S_2)$ co-ordination mode. Apart from **10d** which exhibits rather long Zn–N distances, d(Zn–N) ranges from

Table 2
Selected structural parameters describing the $Zn(N_2S_2)$ co-ordination mode in mono-nuclear tetraco-ordinate complexes

Compound	d(Zn–S)	d(Zn–N)	a(S–Zn–S)	a(N–Zn–N)	$a(ZnN_2S_2)$[a]	References
$Zn(L^{1b})_2$, **7a**	2.297(4)	2.063(10)	137.1(2)	122.7(6)	79.5	[88]
$Zn(L^{1c})_2$, **7b**[b]	2.253(8)–2.274(7)	2.10(2)–2.16(2)	141.1(3)/142.3(4)	115.5(8)/116.6(7)	77.5/78.7	[73]
$Na_2[Zn(L^{2a})_2]\cdot 6H_2O$, **8a**[b]	2.283(1)–2.296(1)	2.046(3)–2.064(3)	132.0(1)/133.4(1)	108.6(2)/116.3(2)	76.2/73.5	[89]
$Zn(L^{2c})_2$, **8b**	2.273(1)	2.090(1)	124.6(1)	104.6(1)	68.3	[89]
$Zn(L^{2d})_2$, **8c**	2.276(2)/2.327(2)	2.021(5)/2.076(6)	127.9(1)	117.6(2)	74.0	[26]
$Zn(L^{3a})_2$, **9a**	2.249(1)/2.257(1)	2.060(3)/2.080(4)	135.6	106.1	70.9	[90]
$Zn(L^{3b})_2$, **9b**	2.247/2.260	2.114/2.121	132.5	95.6	65.1	[91]
$Zn(L^{5a})_2$, **10a**	2.238(2)/2.261(2)	2.105(4)/2.118(4)	123.6(1)	115.1(2)	68.4	[30]
$Zn(L^{5b})_2$, **10b**	2.275	2.108	123.4	116.6	69.3	[31]
$Zn(L^{5c})_2$, **10c**	2.264(2)/2.266(2)	2.062(5)/2.089(5)	123.4(1)	106.9(2)	65.8	[92]
$Zn(L^{5d})_2$, **10d**	2.235/2.276	2.140/2.209	120.4	102.2	59.2	[33]
$Zn(L^{8a})_2$, **11a**	2.258	2.053	139.0	114.6	75.2	[93]
$Zn(L^{8c})_2$, **11b**	2.257/2.262	2.068/2.092	127.4	106.1	67.6	[35]
$Zn(L^{8e})_2$, **11c**	2.269	2.122	118.4	94.4	51.8	[93]
$Zn(L^{8g})_2$, **11d**	2.261/2.263	2.097/2.100	130.5	107.7	69.0	[94]
$Zn(L^{8h})_2$, **11e**	2.228/2.263	2.084/2.115	136.6	104.4	71.3	[95]
$Na_2[Zn(L^{8j})_2]\cdot 2H_2O$, **11f**	2.274	2.060	134.2	116.2	72.2	[41]
$Zn(L^{8l})_2$, **11g**	2.274	2.022	140.8	101.9	71.3	[43]
$Zn(L^{10a})_2$, **12**	2.255(1)	2.114(2)	132.2(1)	99.9(1)	71.3	[86]
$Zn(L^{11})_2$, **13**	2.262(1)/2.265(1)	2.047(3)/2.067(3)	132.1(1)	114.9(1)	72.6	[49]
$Zn(L^{12})_2$, **14**	2.246(1)/2.261(1)	2.068(2)/2.099(2)	127.7(1)	82.6(1)	75.5	[50]
$Zn(L^{22f})$, **15a**	2.253(1)	2.101(2)	140.4(3)	85.6(1)	71.0	[96]
$Zn(L^{22g})$, **15b**	2.253(1)/2.253(1)	2.088(1)/2.128(1)	134.4(1)	85.2(1)	63.4	[96]

[a] $a(ZnN_2S_2)$ denotes the angle between the ZnS_2 and the ZnN_2 plane.

[b] Structure contains two crystallographically different Zn atoms with the same co-ordination mode.

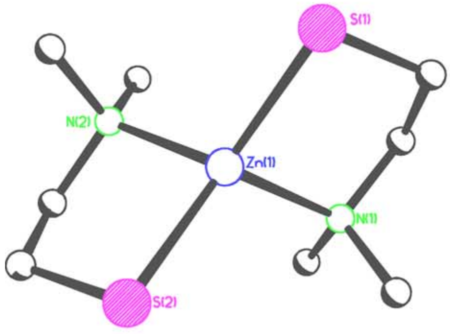

7b

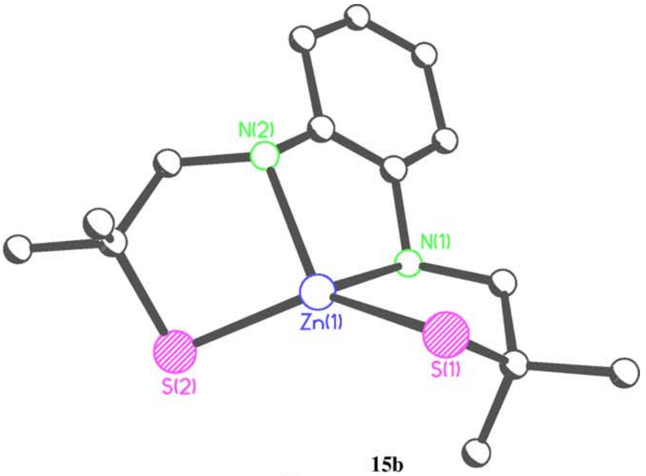

15b

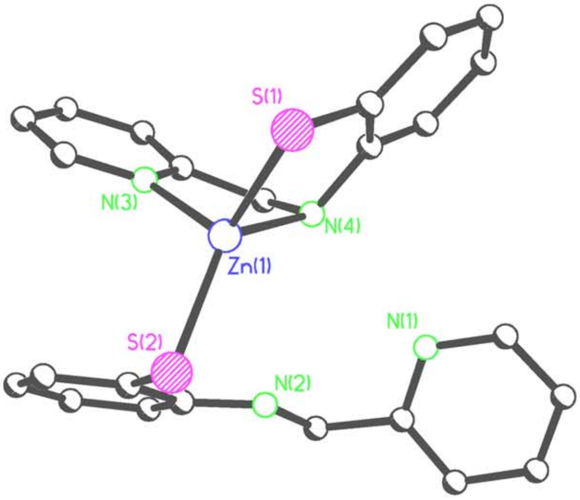

14

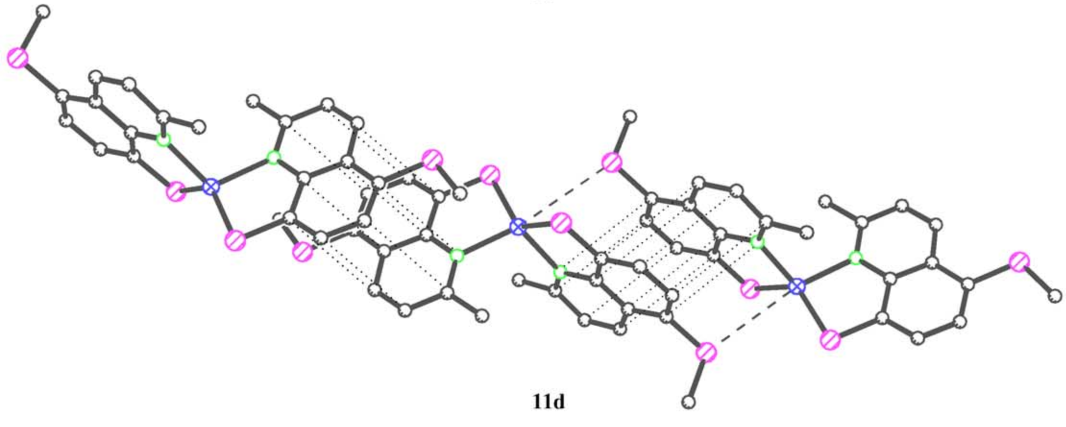

11d

Fig. 2. Molecular structures of selected mono-nuclear Zn^{II} complexes displaying $Zn(N_2S_2)$ co-ordination mode. All H atoms are omitted for clarity. For **11d**, crystal packing is displayed, showing π contacts (dotted lines) and Zn···S interactions between neighboring molecules.

2.02 to 2.16 Å and thus varies a bit more than *d*(Zn–S). In spite of the presence of further donor atoms within the ligand set, no additional contacts to the central ion are found in **8a**, **8b**, **8c**, **12** or **13**. However, such contacts do occur between the SMe substituent of L^{8g} and Zn^{2+} of adjacent molecules in **11d** (see Fig. 2). The structure of $Zn(L^{1b})_2$, **7a**, is nearly identical to that of $Co(L^{1b})_2$ [87], demonstrating that Co^{II} is a suitable analytic probe for Zn^{II} in these N,S-complexes.

3.2.1.2. *Oligo- or poly-nuclear Zn^{II} complexes displaying a $Zn(N_2S_2)$ co-ordination mode.*

Such oligo- or poly-nuclear structures occur if the number of donor atoms available for a chelating or terminal co-ordination per Zn^{2+} is less than

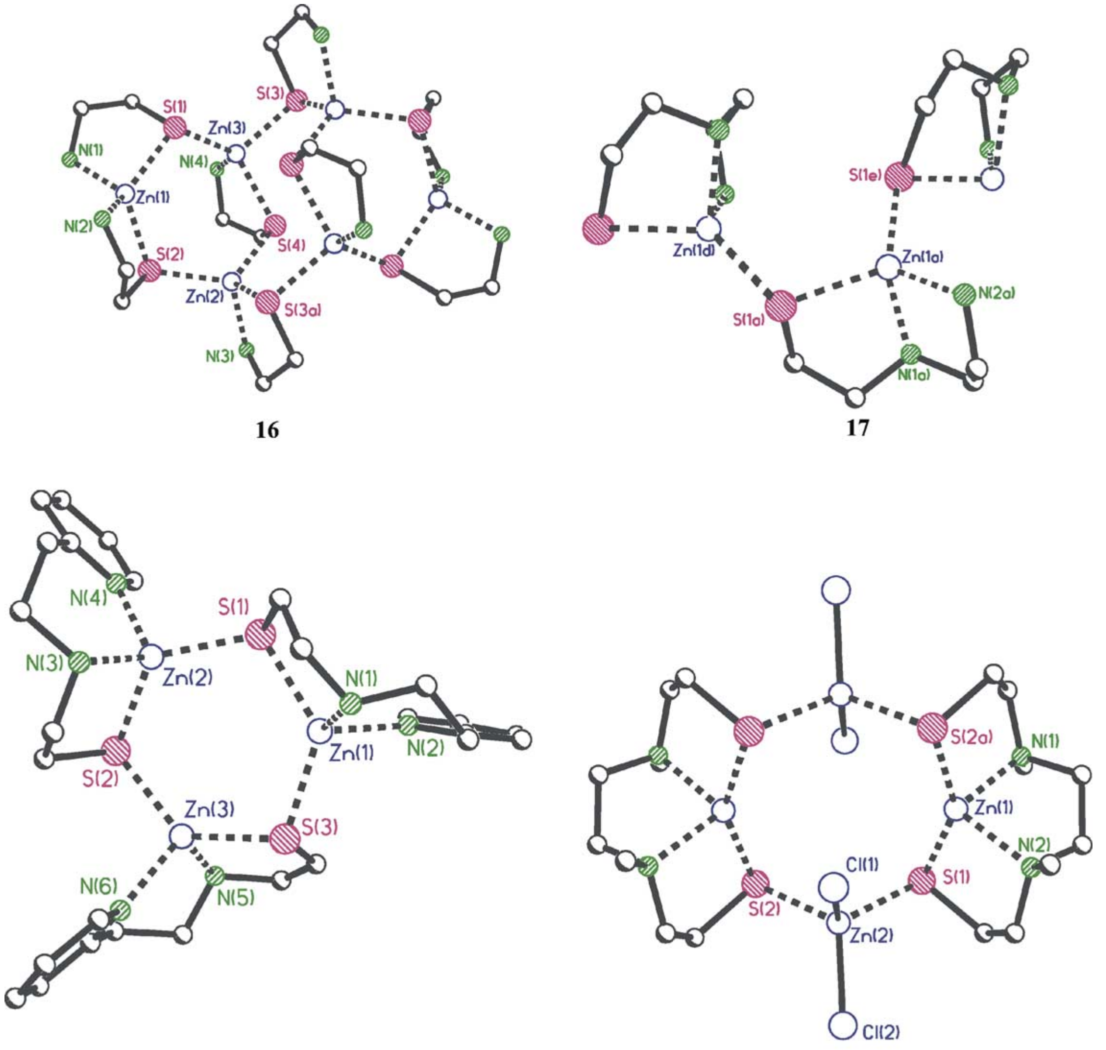

16 **17**

18 **19**

Fig. 3. Molecular structures of oligo- or poly-nuclear Zn^{II} complexes displaying a $Zn(N_2S_2)$ co-ordination mode. All H atoms are omitted for clarity.

four. In these cases, mono-nuclear complexes ligated by 2-aminoethanethiolate (L^{1a}) are available as metalloligands for construction of S-bridged poly-nuclear homo- or heterometallic structures [97–100].

In the hexa-nuclear complex cation of **16** (see Fig. 3) two Zn^{2+} ions (Zn(1) and Zn(1a)) bind to two 2-aminoethanethiolate ligands each and form tetrahedrally co-ordinate $Zn(L^{1a})_2$, the structural data of which is given in Table 3. Each of the remaining four Zn^{2+} ions (Zn(2), Zn(2a), Zn(3), and Zn(3a)) is chelated by one aminothiolate ligand and bridged by two S atoms, forming tetrahedral $[Zn(L^{1a})(\mu\text{-}S)_2]$ units, the structural data of which are given in Table 4. The Zn_6S_8 framework consists of two symmetry related, six-membered Zn_3S_3 rings with boat conformation which are connected via two S atoms such that a centrosymmetric eight-membered ring with chair conformation is formed (see Fig. 3). It is interesting to note that the corresponding Pd-complex, in which the Pd^{2+} ions display a square pla-

Table 3
Selected structural parameters describing the $Zn(N_2S_2)$ co-ordination mode in oligo- or poly-nuclear tetraco-ordinate complexes exhibiting μ^2-bridging S atoms

Compound	*d*(Zn–S)	*d*(Zn–N)	*a*(S–Zn–S)	*a*(N–Zn–N)	*a*(ZnN_2S_2)	References
$[\{Zn(L^{1a})\}_4\{Zn(L^{1a})_2\}_2](ClO_4)_4\cdot 2MeCN$, **16**	2.301/2.324	2.036/2.038	122.7	110.0	69.3	[101]
$[Zn(L^{9a})]ClO_4$, **17**	2.283(2)/2.301(2)	2.045(7)/2.098(7)	117.3(1)	85.8(1)	75.7	[102]
$[Zn_3(L^{10c})_3](ClO_4)_3\cdot CH_3OH$, **18**[a]	2.291–2.312	2.028–2.062	123.2–129.3	98.4–100.6	78.1/79.2	[102]
$[\{ZnCl_2\}_2\{Zn(L^{22b})\}_2]\cdot 2H_2O$, **19**	2.284(4)/2.286(4)	2.08(1)/2.10(1)	148.1(2)	87.0(4)	75.2	[61]

[a] Structure contains three crystallographically different Zn atoms with the same co-ordination mode.

Table 4
Selected structural parameters describing the Zn(N_xS_yX) co-ordination mode in mono- and oligo-nuclear tetraco-ordinate complexes

Compound	CM(Zn)	*d*(Zn–S)	*d*(Zn–N)	*d*(Zn–X)	References
H_3C-Zn(L^{10d}), **20a**	N_2SC	2.297	2.120/2.161	1.986	[104]
[Zn(L^{10d})]O_2CCH_3, **20b**	N_2SO	2.255	2.054/2.132	2.005	[104]
[Zn(L^{10d})]SCN, **20c**	N_3S	2.241	2.021/2.086	1.961	[48]
[Zn(L^{10d})]Br, **20d**	N_2SBr	2.255(1)	2.058(2)/2.110(2)	2.378(1)	[48]
[Zn_4(L^{18c})$_4$], **21**[a]	NS_3	2.251(4)–2.357(3)	2.109(3)–2.161(4)		[106]
[Zn_4(L^{19})$_4$], **22**[b]	NS_3	2.264(3)–2.363(3)	2.089(8)/2.101(8)		[58]
[{*Zn*(L^{1a})}$_4${Zn(L^{1a})$_2$}](ClO_4)$_2$·2MeCN, **16**	NS_3	2.313–2.366	2.038/2.087		[101]

[a] Zn–S distances within chelating ring are shorter (2.251(4)–2.272(4) Å) than those between different molecules (2.313(3)–2.357(3) Å).

[b] Zn–S distances within the chelating ring are shorter (2.264(3)/2.277(3) Å) than those between different molecules (2.314(3)/2.363(3) Å).

nar configuration, forms a hexa-nuclear [{Pd_2{Pd(L^{1a})$_2$}$_4$]$^{4+}$ complex with a pin-wheel type structure.

18 was formed by reaction of Zn(ClO_4)$_2$ with equal amounts of HL^{10c} and NEt_3 in an acetonitrile–methanol mixture. The central structural unit of the trivalent complex cation is a Zn_3S_3 ring which is slightly ruffled in the direction of a boat conformation (see Fig. 3). It contains three crystallographically different Zn(N_2S_2) atoms. All endocyclic Zn–S bonds are of similar length and there is no significant difference between Zn–N distances. In **16** and **18**, μ^2 co-ordination mode of the S atoms is obviously preferred over binding of MeOH, MeCN or ClO_4^- to Zn^{2+}.

The tetra-nuclear [{$ZnCl_2$}$_2${Zn(L^{22b})}$_2$] neutral complex of compound **19** consists of a centrosymmetric eight-membered Zn_4S_4 ring exhibiting two types of differently co-ordinated Zn^{2+} ions. Apart from the Zn(N_2S_2) moiety, the structure of which is described in Table 3, there are also Zn^{2+} ions with a Zn(Cl_2S_2) co-ordination mode present in **19** (see Fig. 3). Both display a distorted tetrahedral co-ordination mode, but the Zn–S distance is significantly longer in the latter (2.343(3) and 2.256(3) Å) than in the former. All Zn–S–Zn bridges are rather symmetric, *d*(Zn–S) being on average about 0.04 Å longer than in the mono-nuclear complexes. Accordingly, the Zn–N distances are on average shorter than in the mono-nuclear analogues.

In contrast to **16**, **18** and **19**, **17** forms an infinite polymeric chain via μ^2 bridging S atoms (see Fig. 3), in which only one type of Zn(N_2S_2) co-ordinated Zn^{2+} ions are present.

3.2.1.3. Mono- or oligo-nuclear tetraco-ordinate Zn^{II} complexes displaying a Zn(N_xS_yX) co-ordination mode.

In this section, tetraco-ordinate Zn^{II}-complexes with N,S-ligands not having a Zn(N_2S_2) co-ordination mode are presented. In the enzymes liver alcohol dehydrogenase [83], spinach carbonanhydrase [84], and peptide deformylase [103], Zn^{2+} ions are tetraco-ordinate and bind to cysteine and histidine, displaying a Zn(NS_2X) co-ordination mode. In these cases, X describes a H_2O molecule, an –OH group or the reaction substrate. The complexes dealt with in this section are model compounds for these types of enzymes.

20a was prepared by reaction of Zn(CH_3)$_2$ with HL^{10d}. According to the Cambridge Crystallographic Database, it is so far the only reported structure of an (N_2S)zinc–alkyl complex. It exhibits a distorted tetrahedral arrangement of the ligands around the Zn-center (see Fig. 4). The Zn–C bond length for **20a** is not much different from that observed for tetraco-ordinate (N^3)Zn–CH_3 compounds (N_3 = substituted tris(pyrazolyl)borate) and it was inferred that the Zn–C dis-

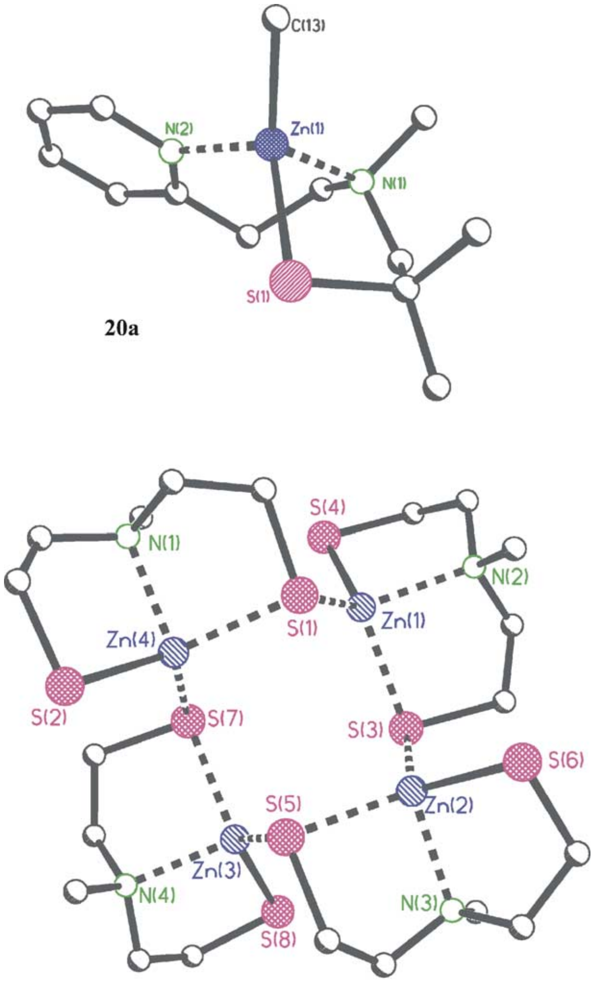

20a

21

Fig. 4. Molecular structures of selected mono- or oligo-nuclear tetraco-ordinate Zn^{II} complexes displaying a Zn(N_xS_yX) co-ordination mode. All H atoms, and in **21** all C atoms of phenyl rings are omitted for clarity.

Table 5

Selected structural parameters describing the $Zn(N_xS_yX_z)$ co-ordination mode in mono- and oligo-nuclear pentaco-ordinate complexes

Compound	CM(Zn)	*d*(Zn–S)	*d*(Zn–N)	*d*(Zn–X)	τ[a]	References
$[Zn_4(L^{25})_2$-μ^3-$(OR)_2]$, **23**[b,c]	NSO_3	2.382(2)/2.389(2)	1.999(5)/2.001(5)	2.014(4)–2.096(4)	0.055/0.061	[68]
	NS_2O_2	2.291(2)–2.383(2)	2.079(5)/2.084(5)	2.151(4)–2.172(4)	0.288/0.286	
$[Zn(L^{13})(HOCH_2CH_2NH_2)]$, **24**	N_2SO_2	2.314(4)	2.19(1)/2.20(1)	1.95(1)/2.08(1)	0.842	[51]
$[Zn(L^{10a})(2$–O_2C–$C_{10}H_6N)]$, **25**	N_3SO	2.285(1)	2.104(3)–2.220(4)	2.015(2)	0.745	[86]
$[Zn(L^{16c})(2,2'$-bipy$)]$, **26**[b]	N_3SO	2.327(4)–2.340(4)	2.097(8)–2.150(9)	1.939(8)/1.950(8)	0.543/0.545	[55]
$[Zn(L^{21})OAc]$, **27**	N_3SO	2.272	2.098–2.287	1.946		[108]
$[Zn(L^{20})Cl]$, **28**	N_3SCl	2.303(1)	2.113(3)–2.313(3)	2.337(1)	0.815	[59]
$[Zn(Tp^{Cum,Me})(L^{2c})]$, **29**[d]	N_4S	2.257(2)–2.276(3)	2.055(6)–2.368(8)		0.527/0.595	[109]
$[Zn(L^{10a})OAc]$, **30**	N_2S_2O	2.378(1)/2.485(1)	2.155(2)/2.183(2)	2.001(2)	0.148	[86]
$[Zn(L^{10a})Cl]$, **31**	N_2S_2Cl	2.385(1)/2.403(1)	2.138(2)/2.235(2)	2.418(1)	0.687	[86]
$Zn(L^{23a})$, **32a**	N_3S_2	2.308(1)/2.340(1)	2.133(3)–2.274(4)		0.602	[110]
$Zn(L^{23b})$, **32b**	N_3S_2	2.329(1)/2.337(1)	2.142(4)–2.179(3)		0.765	[110]
$Zn(L^{24a})$, **33a**	N_3S_2	2.30(1)/2.31(1)	2.00(2)–2.32(2)		0.475	[66]
$Zn(L^{24b})$, **33b**	N_3S_2	2.331(3)–2.339(2)	2.117(6)–2.170(7)		0.335	[111]
$Zn(L^{22h})$, **34**	N_2S_3	2.327(1)–2.494(1)	2.231(2)–2.255(2)		0.310	[112]

[a] $\tau = (a_1 - a_2)/60$, with a_1 and a_2 being the largest and second largest of all X^1–M–X^2 angles around pentaco-ordinate metal center M, respectively. $\tau = 1$ for an ideal trigonal bipyramid ($a_1 = 180.0$, $a_2 = 120.0$), while $\tau = 0$ for a square pyramid ($a_1 = a_2$) [107].

[b] Structure contains two independent molecules in the unit cell.

[c] R = $-CH_2C_6H_4(4\text{-}CF_3)$.

[d] Tris(pyrazolyl)borate ligand in which C atoms adjacent to N atoms carry methyl and cumyl substituents.

tance is insensitive to the other ligands of the co-ordination sphere [104].

The synthesis of **20b** was accomplished by reaction of **20a** with formic acid in CH_2Cl_2. The Zn–S and Zn–N distances are slightly shorter in **20b** than in **20a**. According to structural criteria laid down by Kleywegt et al. [105], the co-ordination mode of the formate ligand is just on the borderline between monodentate and anisobidentate, i.e. the Zn atom could also be described as pentaco-ordinate.

20c and **20d** were obtained by reaction of HL^{10d} with $Zn(SCN)_2$ and $ZnBr_2$, respectively. According to Chang et al., the two methyl groups on the C atom in α-position to the sulfur atom are essential in order to obtain mono-nuclear complexes and to avoid a μ^2-bridging S atom [48].

21 (see Fig. 4) and **22** both contain eight-membered Zn_4S_4 ring structures with $Zn(NS_3)$ co-ordination modes, but with different types of ring conformation. While the one in the latter compound displays a centrosymmetric chair conformation with two crystallographically different Zn^{2+} ions, the former has a boat conformation with slight deviation from C_2-symmetry and consequently four crystallographically different Zn^{2+} ions. The structural parameters of the two are rather similar, the Zn–N distances are slightly longer in the former. A $Zn(NS_3)$ co-ordination mode is also present in compound **16**.

3.2.1.4. *Mono- and poly-nuclear pentaco-ordinate Zn^{II} complexes displaying a $Zn(N_xS_yX_z)$ co-ordination mode.*

There are several examples of pentaco-ordinate Zn^{II}-complexes with 2-amino or 2-iminothiolate ligands. The kinds of co-ordination mode as well as the configuration of the donors around the Zn^{II} depend on the ligand(s). The structural parameter, $\tau = (a_1 - a_2)/60$ is a measure for the continuous transition from a tbp ($\tau = 1$) to a sp ($\tau = 0$) configuration, with a_1 and a_2 being the largest and second largest of all X–Zn–Y angles [107]. In addition to the original definition, it should be noted that τ adopts small values for a distortion from tbp to an edge capped tetrahedron, too. The capped tetrahedron and the sp configuration can be distinguished as follows: if X is the capping atom, two X–Zn–Y angles are smaller and two larger than 90°. In contrast, if X is the apex atom in a sp configuration, all X–Zn–Y angles are larger than 90°. Additionally to τ, the Zn–S, Zn–N and Zn–X distances are used to describe the co-ordination geometry (see Tables 5 and 6).

As was found for the tetraco-ordinate Zn^{II} complexes (vide infra), the Zn–S distances to bridging S atoms are on average bigger than those to terminally co-ordinating S atoms.

In most cases of tbp complexes with N_2S ligands having aromatic and aliphatic N atoms, the aromatic N atoms prefer the equatorial positions while the aliphatic N atoms occupy the apical positions. There are, however, some notable exceptions.

Within the $Zn(N_3SO)$ and $Zn(N_3S_2)$ complexes with tbp configuration, always two N atoms occupy the apical positions, while in the case of $Zn(N_3SCl)$ configuration, one N and one Cl atom are in the apical sites.

23 contains two differently co-ordinate Zn^{2+} ions, both exhibiting a sp geometry (see Fig. 5). At the $Zn(NSO_3)$ co-ordinate Zn(1) atom O(2a) takes the apex position while in the $Zn(NS_2O_2)$ co-ordinate Zn(2) atom, S(1) is in that place instead and deviation from ideal sp geometry is larger here.

Two different ligands ensure a high geometrical flexibility in the mono-nuclear complex of **24** (see Fig. 5). The co-ordination geometry around the Zn^{2+} ion is a slightly distorted trigonal biypramid, where N(1) atoms occupy the apical positions with a nearly linear N–Zn–N arrangement. Since Zn–O1 is 0.13 Å shorter than Zn–O2, it can be assumed that O2 is protonated and O1 is not.

Table 6
Selected structural parameters describing the $\mathrm{Zn(N_4S_2)}$ co-ordination mode in hexaco-ordinate complexes

Compound	*d*(Zn–S)	*d*(Zn–N)	*a*(S–Zn–S)	*a*(N–Zn–N)	References
$[\mathrm{Zn\{Zn(L^{9a})\}_2](ClO_4)_2}$2.5MeCN, **35**[a]	2.593(6)–2.656(6)	2.11(1)–2.14(2)[b] 2.17(2)–2.21(2)[c]	86.9(2)/87.5(2)	178.8(6)/179.0(7)[b]	[102]
$[\mathrm{Zn\{Zn(L^{10a})\}_2](ClO_4)_2}$2MeOH, **36a**[a]	2.538(3)–2.596(3)	2.129(8)–2.168(6)[b] 2.212(6)–2.249(7)[c]	89.5(1)/90.1(1)	177.3(3)/177.8(4)[c]	[102]
$[\mathrm{Zn\{Zn(L^{10a})\}_2](BF_4)_2 2H_2O}$, **36b**[a]	2.564(3)/2.602(3)	2.112(7)/2.133(8)[b] 2.182(8)/2.259(8)[c]	86.6(1)/89.8(1)	178.2(4)/179.8(4)	[86]
$[\mathrm{Zn\{Zn(L^{10b})\}_2]I_2}$, $\mathrm{3Me_2SO}$ **36c**	2.545(3)	2.148(3)[b] 2.230(9)[c]	89.5(1)	176.0(3)	[47]
$[\mathrm{Zn\{Zn(L^{10b})_2\}](MeSO_4)_2}$, **36d**[a]	2.552(1)/2.555(1)	2.155(3)/2.180(3)[b] 2.224(3)/2.225(3)[c]	90.3(1)/90.8(1)	176.5(1)	[47]

[a] There are two crystallographically independent Zn atoms displaying a $(\mathrm{N_4S_2})$ co-ordination mode.
[b] Zn–N bonds with mutual *trans* position.
[c] Zn–N bonds *trans* to Zn–S bonds.

Two different ligands—one tri- and one bidentate—form a distorted trigonal biypramidal co-ordination sphere around the $\mathrm{Zn^{2+}}$ ion of **25**. The mono-nuclear complex displays a $\mathrm{Zn(N_3SO)}$ co-ordination mode. The N atom of 2-carboxyquinoline and the aliphatic N atom of $\mathrm{L^{10a}}$ occupy the apical positions, with *a*(N–Zn–N) = 170.5(1)°. As expected, the apical Zn–N distances (2.180(3) and 2.220(4) Å) are longer than the equatorial one. The sum of the equatorial angles amounts to 359.3°, i.e. the Zn atom lies in the equatorial plane.

26 (see Fig. 5) was prepared electrochemically via simultaneous anodic oxidation of Zn and cathodic reduction of the disulfide form of the ligand. The two crystallographically independent molecules exhibit configurations which are midway between tbp and sp, as can be seen from τ. In a tbp description, N(1) and N(2) occupy the apical positions, with *a*(N–Zn–N) = 175.1(3) and 176.3(3)°, respectively, and a rather large equatorial S–Zn–O angle of 142.4(3) and 143.7(3)°, respectively. The sum of equatorial angles is 359.8°, the $\mathrm{Zn^{2+}}$ ion being virtually co planar with the equatorial atoms.

27 is formed by a ring opening S–C bond rupture in the ligand precursor 2,6-bis(2-benzothiazolinyl) with $\mathrm{Zn(OAc)_2}$ in acetone/dmf. Its molecular structure is similar to that of **28** (see Fig. 5), which promotes the hydrolysis of phosphate diesters. In the latter, the Zn atom has a slightly distorted trigonal bipyramidal co-ordination, with the sum of the equatorial angles being 347.7° and the Zn atom being displaced out of the $\mathrm{N_2S}$ plane to toward the Cl atom.

29 is a mono-nuclear complex in which the $\mathrm{Zn^{2+}}$ exhibits strong distorted tbp geometry. It is the only example for a metal with $\mathrm{M(N_4S)}$ co-ordination mode. The tridentate $\mathrm{Tp^{Cum,Me}}$ ligand occupies one apical and two equatorial sites, with the N and S donor atoms of $\mathrm{L^{2c}}$ being in the remaining apical and equatorial positions, respectively. The differences in Zn–N between the apical (2.260(7)–2.368(8) Å) and equatorial (2.055(6)–2.076(7) Å) sites are very large. Furthermore, the two crystallographically different molecules show some significant differences in their structural parameters describing the co-ordination to the $\mathrm{Zn^{2+}}$ ion. Interestingly, the space group in which the compound crystallizes is centro-symmetrically, implying that racemization must have occurred in one step of its preparation, since L-cysteine was used as starting material.

30 and **31** are poly-nuclear in the solid state, the individual molecules being connected by μ^2 bridging S atoms. In both compounds the single units are related by a two-fold screw axis. **31** displays a distorted trigonal bipyramidal configuration around the $\mathrm{Zn^{2+}}$ ion. Two S atoms and the aromatic N atoms of the ligand occupy the equatorial positions, the sum of equatorial angles being 356.0°. The Zn atom is thus slightly displaced out of the equatorial plane toward the Cl atom. Since $\mathrm{ClO_4^-}$ is more weakly co-ordinating than $\mathrm{Cl^-}$, **30** does not exhibit a trigonal bipyramidal but rather an O-capped distorted tetrahedral configuration around the $\mathrm{Zn^{2+}}$ ion. Accordingly, the Zn–S and Zn–N distances are shorter and the Zn–O distance is longer as compared to **30**. Small and large S–Zn–N (89.1(2) and 119.8(2)°) and N–Zn–N (85.8(3) and 116.7(2)°) angles demonstrate the deviation from an ideal tetrahedral $\mathrm{Zn(N_2S_2)}$ arrangement.

32a (see Fig. 5) and **32b** both exhibit slightly distorted tbp structures. They differ only in the nature of the N atoms in the apical positions which are of an amine type in **32a** and of an imine type in **32b**. Hence in **32b**, the larger amine N atom occupies the equatorial site, which is usually closer to the central atom than the apical one. Consequently, the differences between equatorial and apical Zn–N distances are small in **32b** as compared to **32a**.

33a and **33b** exhibit distorted tbp co-ordinate Zn atoms, in which distortion is not towards tp but capped tetrahedral, since two of the angles including the apex atom are smaller and two are larger than 90°. The two chelating –NCCN– units in both of the compounds offer less structural flexibility than the $\mathrm{–N(CH_2)_3N–}$ units in **32a** and **32b** and consequently, the deviation from an ideal tbp configuration is larger for **33a** and **33b** than for **32a** and **32b**.

34 (see Fig. 5) forms a centrosymmetric di-nuclear complex with μ^2 bridging S atoms and pentaco-ordinate $\mathrm{Zn^{2+}}$ ions. The configuration around the $\mathrm{Zn^{2+}}$ ion can be described as distorted sp, with S(2a) occupying the apex position of

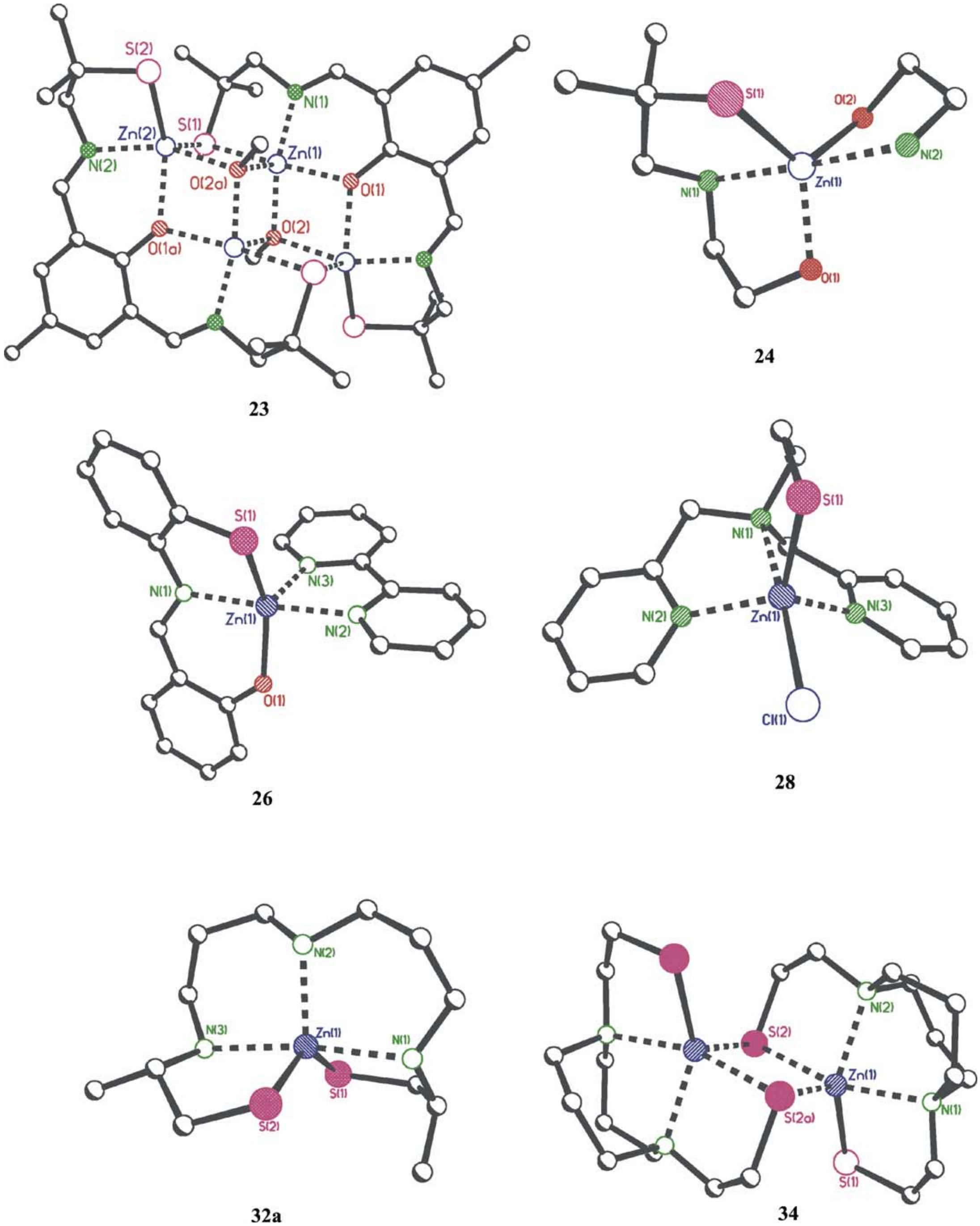

23 **24**

26 **28**

32a **34**

Fig. 5. Molecular structures of selected mono- and poly-nuclear pentaco-ordinate Zn^{II} complexes displaying a $Zn(N_xS_yX_z)$ co-ordination mode. All H atoms are omitted for clarity. For **23**, only the methylene C atom of R binding to O2 is displayed for clarity. For **23** and for **26**, only one of the two crystallograhically independent molecules is shown.

Zn(1). Correspondingly, N(1) and N(2) in the square base show less differences in their distances to the Zn atoms than S(1) and S(2) do.

3.2.1.5. Mono-nuclear Zn^{II} complexes displaying a $Zn(N_4S_2)$ co-ordination mode. All structurally characterised complexes are tri-nuclear with two terminal *cis*-octahedrally $Zn(N_4S_2)$ co-ordinate Zn^{2+} ions (Zn(2) and Zn(3) in Fig. 6), in line with a tetrahedrally $Zn(S_4)$ co-ordinate Zn^{2+} (Zn(1) in Fig. 6). The *trans* influence of the thiolate donor is greater than that of the amine and imine donor, as can be seen from the Zn–N distances *trans* to S and N atoms. *d*(Zn–S) and *d*(Zn–N) vary over more than 0.1 Å, while *a*(S–Zn–S) and the *trans* N–Zn–N angles remain within narrow ranges, being close to 90 and 180°, respectively.

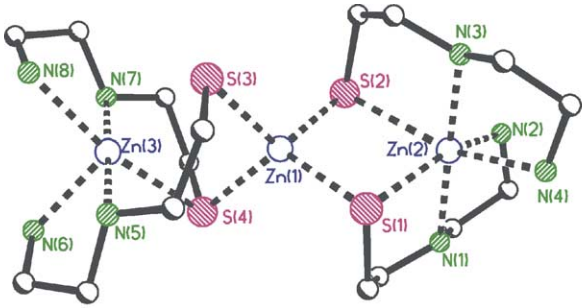

35

Fig. 6. Molecular structure of $[Zn\{Zn(L^{9a})\}_2]^{2+}$, the cation of complex **35**. All H atoms are omitted for clarity.

3.2.2. *Complexes of Cd^{II} and Hg^{II}*

Fewer complexes with N,S-ligands are known of Cd^{II} and Hg^{II} than of Zn^{II}. In contrast to the tetraco-ordinate cases, where Hg^{2+} forms the majority of the structurally characterised complexes, hexaco-ordinate complexes were found only with Cd^{2+}. Except for one case, the tetraco-ordinate complexes exhibit an $M(N_2S_2)$ co-ordination mode with a distorted tetrahedral geometry, while the hexaco-ordinate complexes show a variety of co-ordination modes.

3.2.2.1. Tetraco-ordinate complexes. **37** is a tetra-nuclear complex with a centrosymmetric Hg_4S_4 ring. Similar to **19** (see Fig. 3) and different from the analogous tetra-nuclear Cd^{2+} complexes **43** and **45** (see Section 3.2.2.2. Hexaco-ordinate complexes further down), Hg^{2+} is tetraco-ordinate. Its Hg–S distances and those of **38** (see Fig. 7) are significantly longer than those of the 8-mercaptoquinoline complexes of Hg^{II}. Furthermore, **38** exhibits a much larger N–Hg–N angle than the other compounds.

39a (see Fig. 7) is so far the only structurally characterized tetraco-ordinate Cd^{II} complex with N,S-ligands. There are, however, several Hg^{2+} complexes exhibiting a $Hg(N_2S_2)$ co-ordination mode. The latter significantly differs from that of the Zn and Cd analogues if only complexes with 8-mercaptoquinoline derivatives (HL^{8a}–HL^{8l}) are considered. While d(M–S) increases on average in the sequence M = Zn < Hg < Cd, d(M–N) follows the sequence M = Zn < Cd < Hg. a(S–Hg–S) is much larger than a(S–Zn–S) or a(S–Cd–S) and varies between 147.0° (**39d**) and 164.8° (**39b**). On the other hand, apart from **37** and **38**, a(N–Hg–N) is smaller than 100°. Hence, the geometry of the $Hg(N_2S_2)$ co-ordination resembles a tbp geometry with an unoccupied equatorial site rather than a tetrahedral geometry.

The Hg^{2+} complexes with the 8-mercaptoquinoline ligands exhibit rather similar structures. Nearly all of them display intermolecular π–π-interaction in the solid state, either between quinoline units or, as in **39d**, between the phenyl ring of one ligand and quinoline ring of the other. In $HgPh(L^{8a})$ (data not given in Table 7), a $Hg(NS_2C)$ co-ordination mode is present, with 2.401 and 3.249 Å, for the Hg–S distance within the chelating ring and to the neighboring molecule, respectively [113]. Further intermolecular interaction occurs

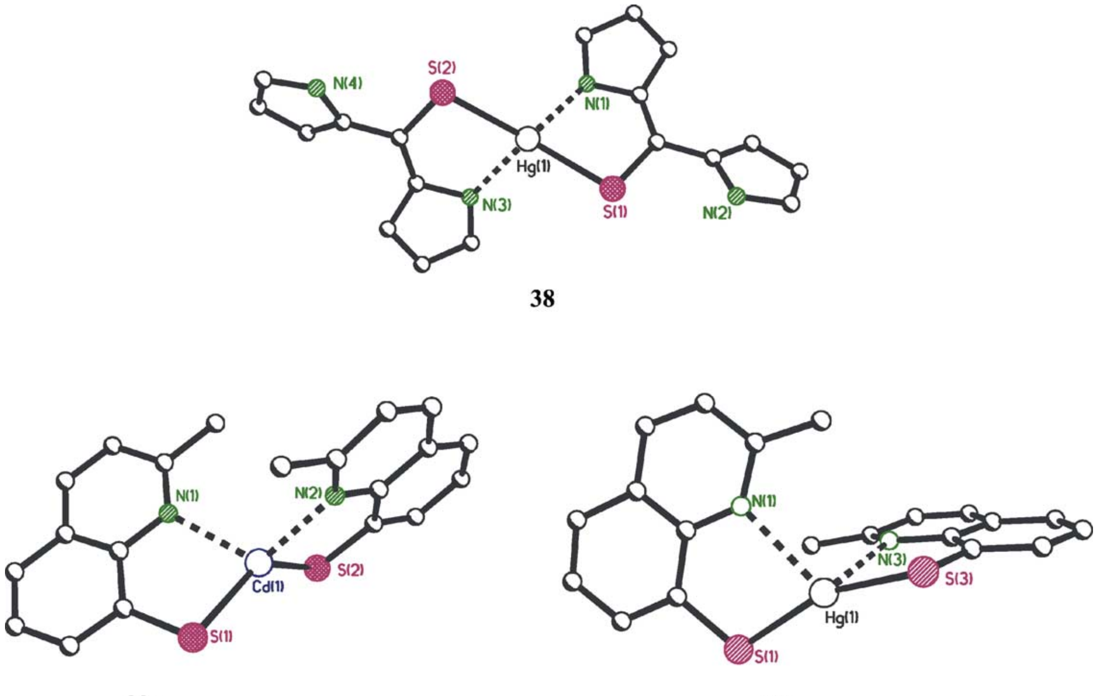

38

39a

39c

Fig. 7. Molecular structures of selected tetraco-ordinate Cd^{II} and Hg^{II}-complexes. All H atoms are omitted for clarity. For **39c**, only one of the two crystallographically different molecules is shown.

Table 7
Selected structural parameters describing the M(N_2S_2) co-ordination mode in mono-nuclear tetraco-ordinate complexes[a]

Compound	*d*(M–S)	*d*(M–N)	*a*(S–M–S)	*a*(N–M–N)	*a*(MN_2S_2)[b]	References
$[\{HgCl_2\}_2\{Hg(L^{1c})_2\}_2]$, **37**	2.414(1)/2.415(1)	2.464(1)/2.506(1)	163.6(1)	117.8(1)	76.2	[114]
$[Hg(L^4)_2]$, **38**	2.450(2)/2.457(2)	2.314(6)/2.330(6)	153.9	129.7	74.0	[115]
$Cd(L^{8b})_2$, **39a**	2.425/2.446	2.288/2.316	134.8	110.5	65.7	[116]
$Hg(L^{8a})_2$, **39b**	2.309/2.325	2.472/2.478	164.8	91.1	68.7	[117]
$Hg(L^{8b})_2$, **39c**[c]	2.334–2.374	2.495–2.608	156.5/158.8	88.8/98.6	62.0/64.9	[34]
$Hg(L^{8e})_2$, **39d**[d]	2.358	2.594	147.0	80.3	46.2	[118]
$Hg(L^{8f})_2$, **39e**	2.342/2.362	2.537/2.564	156.3	98.6	64.1	[119]
$Hg(L^{8k})_2$, **39f**	2.369/2.371	2.482/2.522	155.0	83.3	56.4	[120]
$Hg(L^{8l})_2$, **39g**	2.362/2.366	2.429/2.483	161.4	85.1	63.2	[121]

[a] M = Cd^{II} or Hg^{II}.
[b] Angle between MS_2 and MN_2 planes.
[c] Two independent molecules in the unit cell.
[d] Molecule exhibits C_2-symmetry.

through π-interaction between chinoline rings. Hg–N and Hg–C distances are 2.457 and 2.067 Å, respectively.

3.2.2.2. Hexaco-ordinate complexes. In **41**, the terdentate ligand D-penicillamine displays several co-ordination modes. Apart from the N,S-chelating mode, the S atom acts as μ^2-bridge, as does one of the O atoms of the carboxyl group, while the other O atom binds to a single Cd^{2+}.

47a and **47b** contain tri-nuclear complex cations with a linear arrangement of metal centers. Both are structurally similar to the hexaco-ordinate Zn^{II} complexes with $Zn(N_4S_2)$ co-ordination mode, lacking any co-ordination of the anions to the metal ions. The latter of the two forms in a reaction of one equivalent of $CdCl_2$ with two equivalents of HL^{9b}, i.e. it is preferred over the stoichiometrically feasible complex $Cd(L^{9b})_2$.

HL^7 is the anti-tumor drug 6-mercaptopurine, the synthetic thio analogue of the natural purine hypoxanthine [122]. **42** and **46** (see Fig. 8) are two of its complexes with Cd^{II}. It is interesting to compare the co-ordinating properties of the thione, HL^7, to that of the thiolate form, $(L^7)^-$ (see Scheme 4). Inspite of the increased charge density on the thiolate S-atom compared to the thione S-atom, the Cd−S bond in **42** is significantly shorter than those in **46**. Both compounds exhibit hexaco-ordinate Cd^{2+} ions in centrosymmetric environments. In the former, discrete complex molecules are present, which co-crystallize with two additional molecules of HL^7. In the latter, infinite chains are formed by μ^2 bridging S atoms. Each Cd^{2+} ion in **46** is co-ordinated by four S atoms and two N atoms in *trans* position. The S-bridges are not symmetrical, the Cd(1b)–S(1b) bond within the chelating ring being significantly shorter than the Cd(1b)–S(1c) bond.

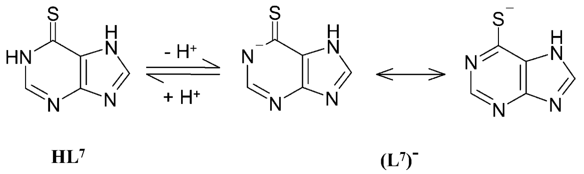

Scheme 4.

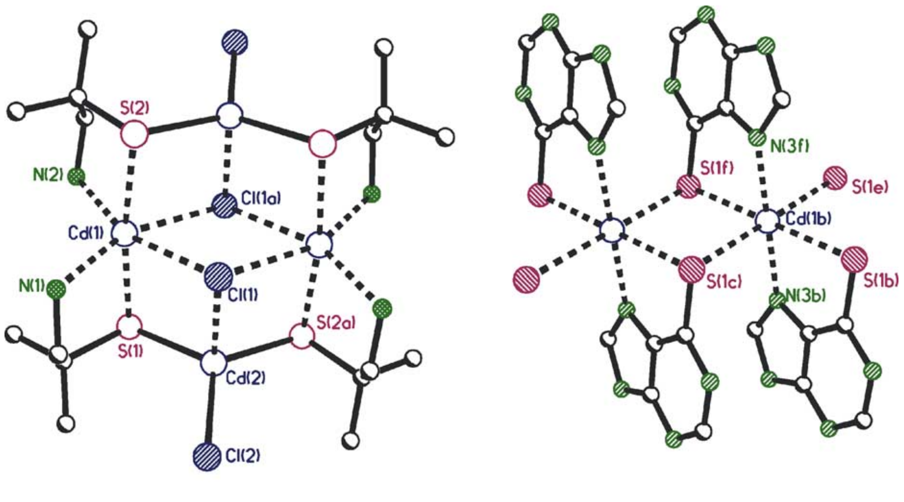

43 **46**

Fig. 8. Molecular structures of selected hexaco-ordinate Cd^{II} complexes. All water molecules and all H atoms are omitted for clarity.

Table 8
Selected structural parameters describing the co-ordination mode in hexaco-ordinate Cd^{II} complexes

Compound	CM(Cd)	*d*(Cd–S)	*d*(Cd–N)	*d*(Cd–X)	Reference
$[Cd(L^{16c})(phen)]_2$, **40**	N_3SO_2	2.530(3)	2.340(8)–2.503(7)	2.270(7)/2.333(6)	[123]
$[Cd(L^{14})]$, **41**	NS_2O_3	2.563(7)/2.567(7)	2.38(2)	2.40(2)–2.57(2)	[124]
$[Cd(HL^7)_2Cl_2]\cdot 2HL^7$, **42**	$N_2S_2Cl_2$	2.622(1)	2.366(1)	2.719(1)	[122]
$[\{CdCl_2\}_2\{Cd(L^{1b})_2\}_2]\cdot 2H_2O$, **43**	$N_2S_2Cl_2$	2.558(4)/2.558(4)	2.35(2)/2.36(2)	2.946(6)/2.946(2)	[125]
$[\{Cd(L^{1c})\}_2\{Cd(L^{1c})_2Cl\}_2]$, **44**	$N_2S_2Cl_2$	2.554(1)/2.559(1)	2.516(3)/2.558(3)	2.733(1)/2.735(1)	[114]
$[\{CdBr_2\}_2\{Cd(L^{1c})_2\}_2]$, **45**	$N_2S_2Br_2$	2.494(2)/2.501(2)	2.366(9)/2.375(9)	3.295(1)/3.369(2)	[114]
$[Cd(L^7)_2]\cdot 2H_2O$, **46**	N_2S_4	2.689(1)[c]	2.868(1)	2.283(3)	[122]
$[Cd\{Cd(L^{9b})\}_2](ClO_4)_2\cdot H_2O$, **47a**	N_4S_2	2.695(3)/2.706(3)	2.371(9)/2.375(9)[a]	2.338(9)/2.385(10)[b]	[126]
$[Cd\{Cd(L^{9b})\}_2]Cl_2 2MeOH$, **47b**	N_4S_2	2.695(4)/2.733(4)	2.37(1)/2.37(1)[a]	2.35(1)/2.35(1)[b]	[126]

[a] Cd–N bonds with mutual *trans* position.
[b] Cd–N bonds *trans* to Cd–S bonds.
[c] S atom within chelating ring.

43 (see Fig. 8), **44**, and **45** contain tetra-nuclear complex molecules. In either case, eight-membered centrosymmetric M_4S_4 (M = Zn, Cd, Hg) rings are present, similar to those in compounds **19** and **37**. Concerning the intramolecular secondary $M \cdots X$ interaction, (X = Cl, Br) there is a gradual change from rather short Cd–Cl distances in **44**, giving a genuine hexaco-ordinate Cd^{2+} to essentially tetraco-ordinate Zn^{2+} in **19** where $Zn \cdots Cl$ distances of 3.375 and 3.537 Å are close to the sum of the van der Waals radii.

The bi-nuclear complex **40** with two μ^2 bridging O atoms was prepared by anodic oxidation of cadmium metal in acetonitrile solution containing $(HL^{16c})_2$ [which was reduced to $(L^{16c})^-$] and addition of phen to the electrolytic phase. The complex displays a distorted octahedral geometry around the Cd^{2+} ion with *trans* angles between 147.6(2) and 160.4(3)° and *cis* angles between 67.8(3)° (phen bite angle) and 108.8(2)°. The Cd–N distances to the phen ligand are longer than those to L^{16c} and the two Cd–O distances in the bridge are rather similar (Table 8).

3.3. Group 13 complexes

Structurally characterised examples of complexes involving N,S-ligands are know for all group 13 metals. In all cases, the metals are in the trivalent state. Combining hard M^{3+} ions with soft N,S-ligands proved to be synthetically challenging in some cases.

3.3.1. Tetraco-ordinate M^{3+}

Only two examples of tetraco-ordinate M^{3+} are known, both with M = Al. The basic structural parameters describing the environment of the tetraco-ordinate Al center do not differ significantly between **48a** (see Fig. 9) and **48b**. Both were prepared by reaction of equimolar amounts of $Al(^tBu)_3$ and HL^{1c} or HL^{1d}, respectively. The complexes are monomeric in the solid state as well as in solution. This contrasts the analogous donor-substituted alkoxide complexes, which tend to dimerize via μ^2-O bridges [127].

3.3.2. Pentaco-ordinate M^{3+}

49a and **49b** (see Fig. 9) are isomorphous with nearly identical unit cell parameters. Both have only slightly distorted tbp configuration with nearly linear N–M–N arrangements. Al–S and Ga–S distances are similar while Al–N distances are significantly shorter than Ga–N distances, reflecting the weaker Lewis acidity of Ga compared to that of Al. The formation of both compounds using $LiAlH_4$ and $LiGaH_4$, respectively, even with only one equivalent of $HL^{1d}\cdot HCl$ is noteworthy.

The In atom in **50** (see Fig. 9) has a tbp geometry with two S and one Cl atom forming the equatorial plane. The sum of the equatorial angles is 359.9 and 360.0 for the two crystallographically independent molecules, i.e. the In atoms are located on the equatorial plane.

51a (see Fig. 9) and **51b** are isomorphous and both exhibit C_s molecular symmetry due to 50/50 disordering. They display an ideal sp configuration ($\tau = 0$), with the Cl atom in the apex position.

52 is a mono-nuclear complex with sp configuration, one of the S atoms occupying the apex position. The N atoms occupy *cis*-positions in the basal square, the Ga–N bond that is *trans* to the Cl atom being significantly longer than the Ga–N bond *trans* to the S atom. The compound is of medical interest since it can be used as a myocardial perfusion imaging agent [128].

53b also exhibits an sp configuration with the SCN^- ion in the apex position, binding with its N-donor site to the In^{3+}. The respective In–N distance is much shorter (2.127(7) Å) than those from $(L^{22a})^{2-}$ (2.291(6) and 2.331(6) Å). The latter three compounds were studied as radiopharmaceuticals, using the respective complexes with ^{67}Ga and ^{111}In isotopes. It is hence of interest, that these air-stable compounds are stable in aqueous solution at pH = 3, but that hydrolysis with formation of the metal hydroxides takes place at pH > 3 [129,130].

The three alike ligands in **53a** (see Fig. 9) do not all co-ordinate in the same fashion. One binds in a monodentate mode and co-ordinates only with S(3) to the In^{3+}, while the other two are bidentate. The monodentate ligand occupies the apex position in an sp configuration, the distorted N_2S_2 basal square exhibiting a *trans*-configuration.

3.3.3. Hexaco-ordinate M^{3+}

In **54** (see Fig. 10) the carboxyl group co-ordinates in a bidentate mode to the In^{3+}, leading to a strongly dis-

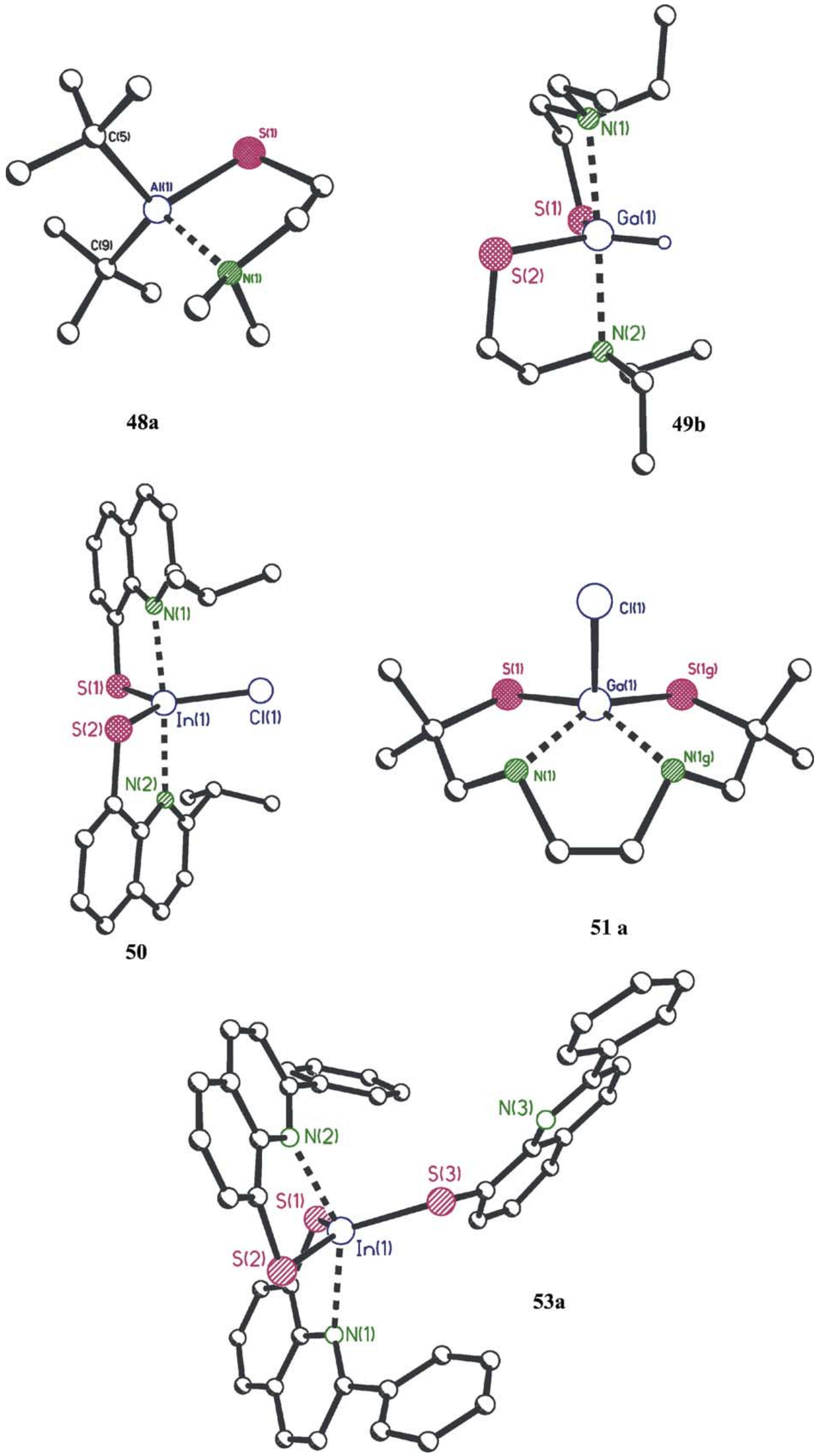

48a

49b

50

51 a

53a

Fig. 9. Molecular structures of selected tetra and pentaco-ordinate group 13 complexes. All H atoms, except that bound to Ga in **49b**, are omitted for clarity.

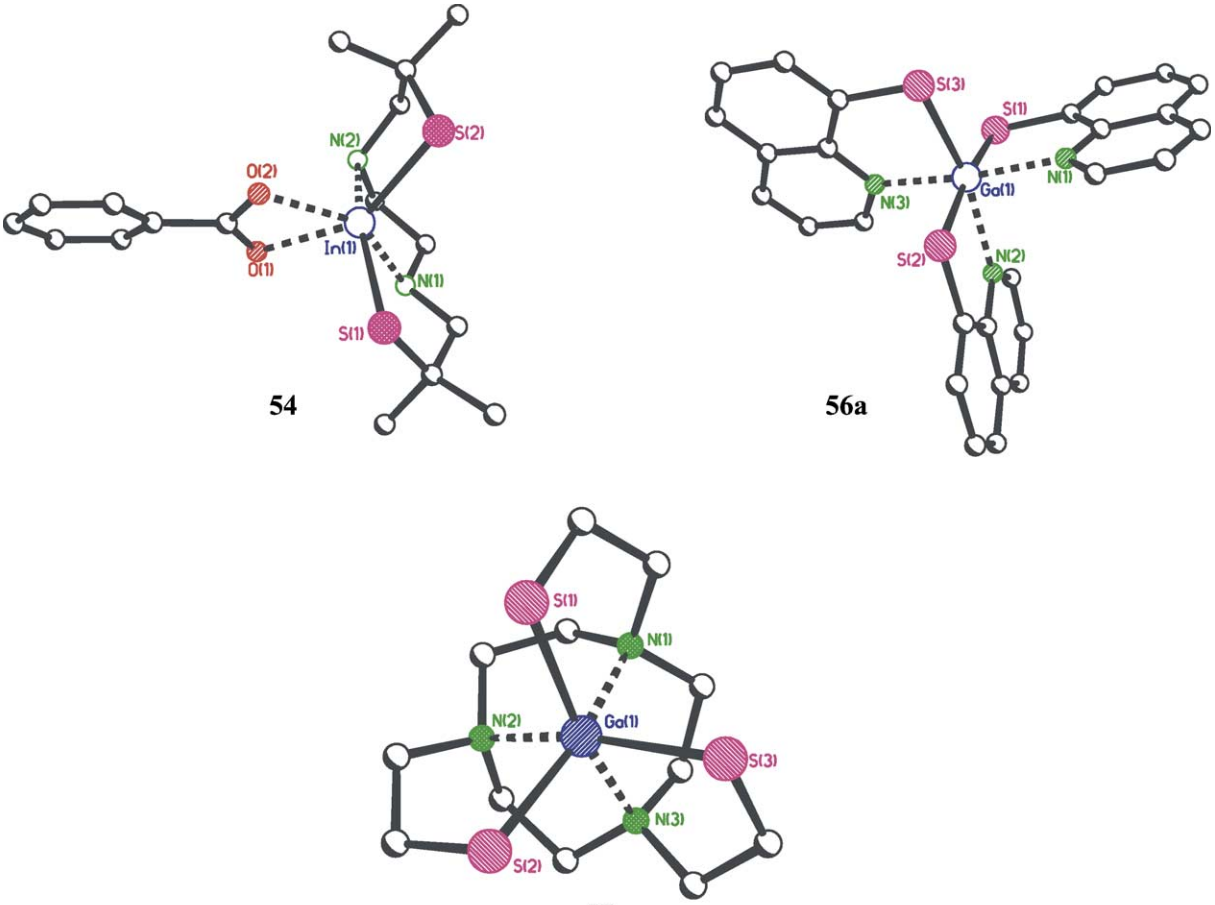

54

56a

57a

Fig. 10. Molecular structures of selected hexaco-ordinate group 13 complexes. All H atoms are omitted for clarity.

torted octahedral configuration with an O–M–O bite angle of 56.3(1)°.

55a and **55b** were prepared from aqueous solutions at neutral pH. In comparison to [Ga(L^{22a})X] and [In(L^{22a})X], the anionic complexes show an increased stability toward hydrolysis (cf. **53b**). They are isomorphous with each other, displaying a distorted octahedral configuration around M^{3+}. The O atoms adopt a *trans* configuration with respect to each other [*a*(O–M–O) = 163.4(5) and 156.3(3) for M = Ga and In].

56a (see Fig. 10), **56b**, **56c**, and **56d** exhibit a *mer*-$M(N_3S_3)$ co-ordination mode. The two shorter M–S bonds (M = Ga, In, Tl) are *trans* to each other, as are the two shorter M–N bonds.

57a (see Fig. 10) was prepared from H_3L^{27a} and $Ga(NO_3)_3$ in ethanol solution, without the use of an additional base to scavenge the HNO_3 that is formed in the course of the reaction. It was subsequently recrystallized from CH_2Cl_2. The complex displays a fully chelated Ga^{3+} in a slightly distorted octahedral environment. **57b** could be obtained by reaction of $InBr_3$ with H_3L^{27a} and NaOEt in ethanol solution. As is the case for **57a**, it shows a hexaco-ordinate M^{3+} in a distorted octrahedral environment (Tables 9–11).

3.4. Group 14 complexes

So far, structurally characterized complexes of Si or Ge with N,S-ligands and E···N interactions (E = Si, Ge) are not known. Tin adopts such complexes in the bi- and tetravalent state while of lead only Pb^{II} complexes are known, presumably due to the high oxidizing power of Pb^{IV} compounds.

Table 9
Selected structural parameters describing the $Al(NSC_2)$ co-ordination mode in tetraco-ordinate Al^{III} complexes

Compound	*d*(Al–S)	*d*(Al–N)	*d*(Al–C)	References
[Al(^{t}Bu)$_2$(L^{1c})], **48a**	2.262(2)	2.044(4)	2.006(5)/2.019(4)	[131]
[Al(^{t}Bu)$_2$(L^{1d})], **48b**	2.272(4)	2.061(7)	2.019(8)/2.020(9)	[131]

Table 10
Selected structural parameters describing the co-ordination in pentaco-ordinate Al^{III}, Ga^{III} and In^{III} complexes

Compound	CM(M)	*d*(M–S)	*d*(M–N)	*d*(M–X)	τ[a]	References
$[AlH(L^{1d})_2]$, **49a**	$Al(N_2S_2H)$	2.271(1)/2.278(1)	2.175(2)/2.182(2)	1.62(2)	0.910	[132]
$[GaH(L^{1d})_2]$, **49b**	$Ga(N_2S_2H)$	2.288(3)/2.289(2)	2.252(9)/2.28(1)	1.33	0.902	[132]
$[In(L^{8d})_2Cl]$, **50**[b]	$In(N_2S_2Cl)$	2.410–2.419	2.375–2.382	2.384/2.391	0.670	[133]
$[Ga(L^{22a})Cl]$, **51a**[c]	$Ga(N_2S_2Cl)$	2.283(2)	2.147(7)	2.241(3)	0.0	[134]
$[In(L^{22a})Cl]$, **51b**[c]	$In(N_2S_2Cl)$	2.440(7)	2.322(10)	2.394(7)	0.0	[134]
$[Ga(L^{22e})Cl]$ dmf, **52**	$Ga(N_2S_2Cl)$	2.247(1)/2.256(1)	2.078(3)/2.204(3)	2.365(1)	0.110	[65]
$[In(L^{8e})_3]$, **53a**	$In(N_3S_2)$	2.427–2.443	2.436–2.513		0.270	[135]
$[In(L^{22a})NCS]$, **53b**	$In(N_3S_2)$	2.411(2)/2.446(2)	2.127(7)–2.331(6)		0.200	[134]

[a] For definition of structural parameter τ in pentaco-ordinate complexes, see Section 1.
[b] Two independent molecule in the asymmetric unit.
[c] The molecules display Cs-symmetry due to disorder.

Table 11
Selected structural parameters describing the co-ordination mode in hexaco-ordinate Ga^{III}, In^{III}, and Tl^{III} complexes

Compound	CM(M)	*d*(M–S)	*d*(M–N)	*a*(S–M–S)	*a*(N–M–N)	References
$[In(C_6H_5CO_2)(L^{22a})]$, **54**	$In(N_2S_2O_2)$	2.454(1)/2.477(1)	2.298(3)/2.367(3)	107.4(1)	76.5(1)	[134]
$Na[Ga(L^{26})]\cdot 2H_2O$, **55a**[a]	$Ga(N_2S_2O_2)$	2.308(4)	2.115(11)	104.8(2)	81.6(7)	[69]
$Na[In(L^{26})]\cdot 2H_2O$, **55b**[a]	$In(N_2S_2O_2)$	2.452(3)	2.281(7)	115.9(1)	77.1(4)	[69]
$[Ga(L^{8a})_3]$ MeOH, **56a**	$Ga(N_3S_3)$, mer	2.331–2.391	2.152–2.310	87.1–171.8	91.5–171.0	[136]
$[In(L^{8a})_3]$ $CHCl_3$, **56b**	$In(N_3S_3)$, mer	2.486–2.530	2.317–2.418	90.6–167.8	90.4–168.9	[137]
$[In(L^{8i})_3]$, **56c**	$In(N_3S_3)$, mer	2.384–2.527	2.359–2.559	96.4–164.6	89.1–167.2	[40]
$[Tl(L^{8a})_3]$, **56d**	$Tl(N_3S_3)$, mer	2.469–2.578	2.491–2.662	97.5–156.7	87.7–170.1	[138]
$[Ga(L^{27a})]$ $2CH_2Cl_2$, **57a**	$Ga(N_3S_3)$, fac	2.335(1)–2.344(1)	2.201(4)–2.221(4)	97.9(1)–98.9(1)	78.9(1)–79.3(1)	[70]
$[In(L^{27a})]$, **57b**[b]	$In(N_3S_3)$, fac	2.499(1)–2.518(1)	2.379(2)–2.408(3)	102.6(1)–106.4(1)	73.8(1)–74.5(1)	[139]

[a] M lays on a C_2 axis.
[b] Structure was also reported in reference [140].

3.4.1. Tetraco-ordinate complexes

58 (see Fig. 11) forms in a photochemical reaction of **62** (see further down) with $Cr(CO)_6$ in thf solution. It is the only complex with a geometry other than tbp. In contrast to the other complexes, the M^{II} atom does not only act as an electron pair acceptor, but as a donor (towards the Cr atom) as well. The stannylene replaces a CO ligand in $Cr(CO)_6$, the Cr–Sn distance being 2.622(1) Å. The geometry of the ligands around Sn^{II} may either be described as a distorted trigonal pyramid or a distorted tetrahedron, the Sn atom being displaced by 0.50 Å from the S_2Cr plane towards the N atom.

In the case of ψ-tbp or ψ-sp geometries and in accordance to the VSEPR rules, the stereochemically active lone pair at the central atom will occupy an equatorial or the apex position, respectively. Since the lone pair (lp) requires more space at the central atom than a covalent or dative single bond, $a(X^{eq}–M–X^{eq}) < 120.0°$ and $a(X^{ap}–M–X^{ap}) < 180.0°$, in a ψ-tbp configuration. Hence, the structural parameter τ may be close to one even for significantly distorted ψ-tbp cases.

59a (see Fig. 11) is one of the few examples of structurally known homoleptic complexes of cysteamine. As well as **60**, **61a**, **61b**, and **61c** it exhibits discrete mono-nuclear units with a distorted ψ-tbp configuration.

59b (see Fig. 12) represents a tri-nuclear complex with Pb^{II} centers in different co-ordination environments. One molecule of **59a**, with $Pb(N_2S_2)$ co-ordination mode and ψ-tbp geometry, co-ordinates with S atoms to the Pb^{II} centers of two $PbCl(L^{1a})$ units. The latter forms additional contacts to neighboring $PbCl(L^{1a})$ units, giving a Pb atom with $Pb(ClNS_3)$ co-ordination mode and distorted ψ-octahedral geometry with significantly different Pb–S distances.

As with $PbCl(L^{1a})$ in **59b**, there are less than four donor atoms per metal atom in **62** (see Fig. 11). Hence, the compound forms a di-nuclear complex in which the two metal centers are bridged by S atoms. Each subunit represents a hetero bicylco$[3.3.0^{1,5}]$ octane system. Two crystallographically different di-nuclear complexes are present in the solid state, one of which is centrosymmetric. This leads to three different Sn atoms, all of which exhibit distorted ψ-tbp configurations, $a(N–Sn\cdots S) = 136.8(1)–151.0(1)$ being the largest of all angles. In all cases, the bridging $Sn\cdots S$ distances are larger than the endo Sn–S bond distances. Note that in the related compound **21**, where $[Zn(L^{18c})]$ units are present, a tetra- instead of a di-nuclear complex is formed.

3.4.2. Complexes with pentaco-ordinate central atoms

63 (see Fig. 12) is a mono-nuclear Sn^{IV} complex, exhibiting a slightly distorted tbp configuration, N(1) and C(7) occupying the apical positions. The Sn(1)–C(7) bond is slightly longer than the equatorial Sn–C bonds. The sum of the equatorial angles is 352.9° and the Sn atom is slightly displaced from the equatorial plane towards C(7).

64a (see Fig. 12) **64b**, **65a**, and **65b** are mono-nuclear Sn^{IV} complexes that all consist of a $[SnR_2]^{2+}$ fragment and

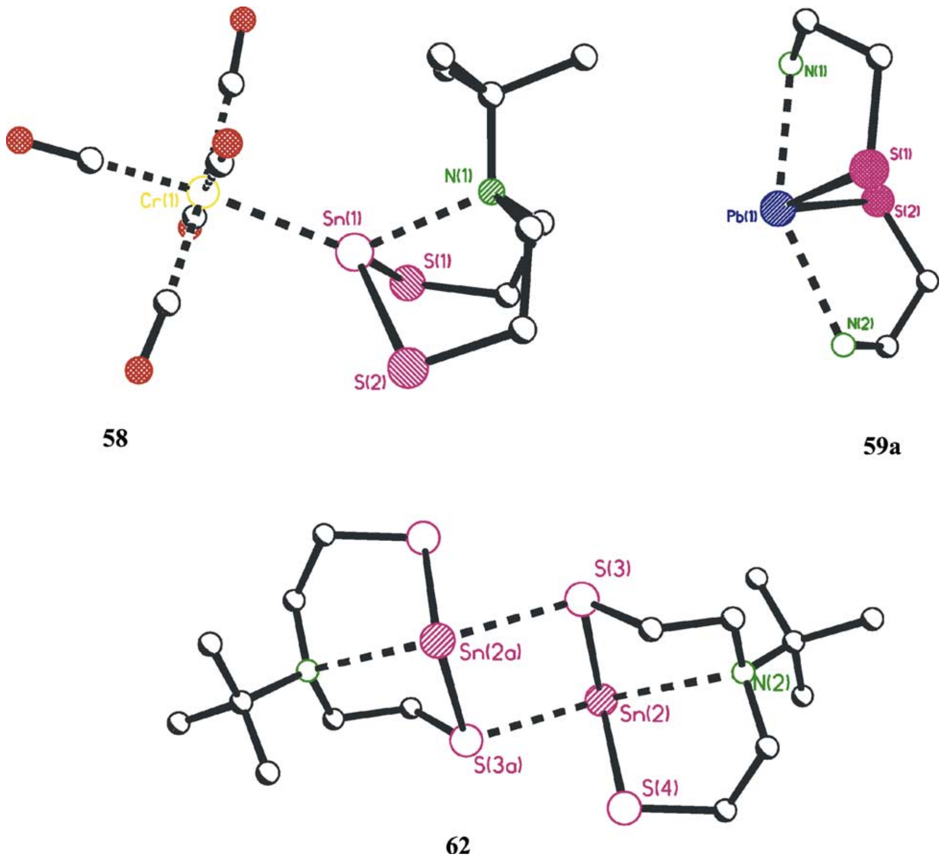

58

59a

62

Fig. 11. Molecular structures of selected tetraco-ordinate group 14 complexes. All H atoms are omitted for clarity. For **62** only one of the two crystallographically independent molecules is shown.

a terdentate $(L)^{2-}$ ligand, with N, S and O donor atoms. Consequently, similar structures arise in all three cases. The τ value demonstrates strongly distorted tbp configurations. The distortion is not towards an sp but towards a distorted edge capped tetrahedron, since the O–M–S angles (158.0(1)°, 157.5(1)°, 158.4° and 161.1(1)°, for **64a**, **64b**, **65a**, and **65b**, respectively) are bent towards and not away from the equatorial N atom. It is noteworthy that O and S instead of N occupy the apical positions. In most cases of N,S-ligands in tbp configured complexes, the N atom is found in the apical and the S atom in the equatorial position. In comparison to the Sn^{IV} complexes with tbp configuration and the N atom in an apical position (e.g. **69a** and **69b**), the Sn–N distances in **64a**, **64b**, **65a**, and **65b** are significantly shorter. The sum of the equatorial angles is 359.6°, 359.3°, 358.9°, and 358.7° for the compounds in the above sequence, i.e. the Sn atoms are located in the equatorial plane in all cases.

N and Cl take the apical positions in the slightly distorted tbp configuration of **66** (see Fig. 12) **67**, and **68**. The respective sums of all equatorial angles amount to 360.0°, 359.3° and 359.8°, i.e. deviation of Sn atom from the SC_2 plane is not significant.

69a (see Fig. 12) contains a terdentate ligand, with two S atoms in the equatorial and the N atom in the apical position. In **69b**, which contains the same ligand and exhibits the same co-ordination modes as **69a**, a CH_2-group bridges two pentaco-ordinate Sn^{IV} centers, both exhibiting tbp configuration. An interesting feature of this solid state structure is the fact that the CH_2 group occupies an equatorial position on one and an apical position on the other Sn atom. The Sn atom with the CH_2 group in equatorial position shows less deviation from an ideal tbp configuration than the Sn atom with the CH_2 group in apical position. On the basis of NMR spectroscopy, several structural isomers of **69b** are in equilibrium with each other in solution [141]. While d(Sn–S) and d(Sn–C) are similar for **69a** and **69b**, d(Sn–N) is significantly smaller for the former, i.e. it has got the stronger donor acceptor interaction between Sn^{IV} and N.

70 is a quite unusual complex. Four Sn^{IV} atoms sitting on the outside of a modified porphyrin ligand, the centre of which contains a Ni^{2+}. Two different types of pentaco-ordinate Sn^{IV} atoms with similar distorted sp configurations and structural parameters are present.

In **71** (see Fig. 12) Pb(1a) has a capped ψ-tbp configuration, which is due to an anisobidentate NO_3^-, taking one of the apical and the capping position. N(1a) resides in the other apical position, while the equatorial sites are occupied by S(1a) and S(1ga). The distance of S(1a) to Pb(1a) is shorter than the Pb(1a)–S(1ga) distance.

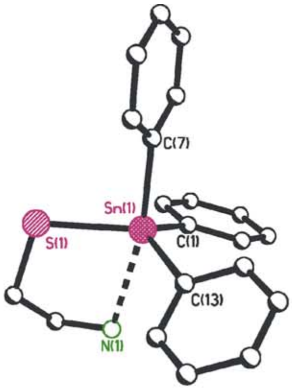

63

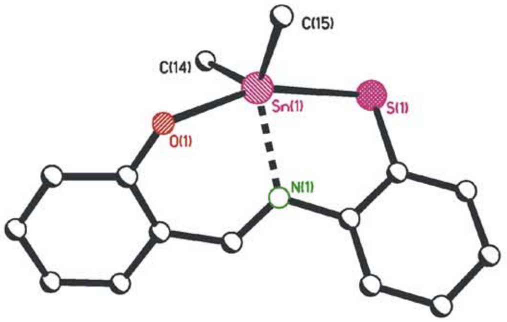

64a

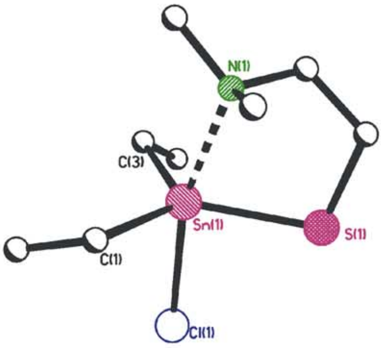

66

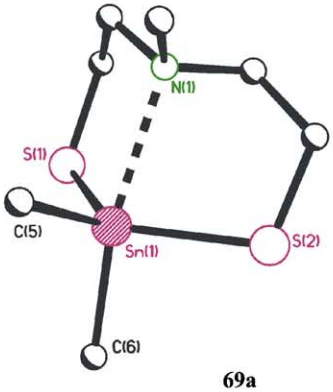

69a

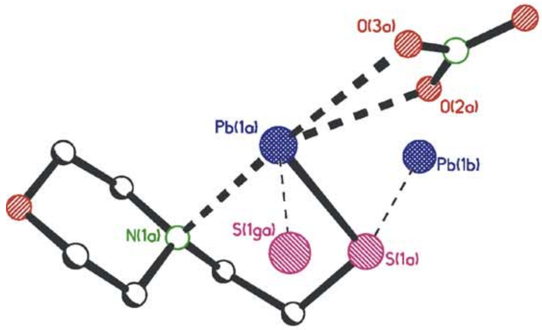

71

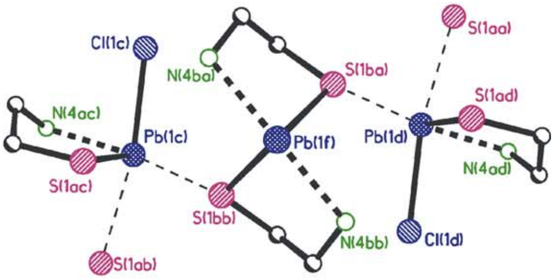

59b

Fig. 12. Molecular structures of selected pentaco-ordinate group 14 complexes. All H atoms are omitted for clarity.

3.4.3. *Complexes with hexaco-ordinate central atoms exhibiting octahedral or ψ-pbp configuration*

72 (see Fig. 13) could be prepared by an oxidative addition of $SnCl_2$ to 2-(2-methoxyphenyl)benzothiazol with a ring opening C–S bond rupture. In the solid state, a centrosymmetric di-nuclear complex is present, with two distorted octahedrally co-ordinate Sn^{IV} centers. Both Sn atoms are bridged by two MeO^- ligands, S(1) and Cl(1) being *trans* to the two O(1) and O(1a), respectively.

73 and **74** (see Fig. 13) were prepared electrochemically and both exhibit Sn^{IV} in distorted octrahedral co-ordination environments. In the former complex, the Sn atom is placed on a centre of inversion while in the latter, the N atoms are *trans* and the other alike donor atoms are *cis* to each other.

75 (see Fig. 13) was obtained from a $SnCl_2$ solution in methanol, to which two equivalents of $[H_2L^{2b}]Cl$ were added and which was exposed to the atmosphere for two days. In the distorted octrahedral complex, S(1) and S(2) are *trans* to each other, while Cl(1) and Cl(2) are in *cis* position, as are N(1) and N(2). Of the two enantiomeric forms of this configuration, only one is present due to the fact that L^{2b} (*O*-methyl-L-cysteinate) is a chiral ligand.

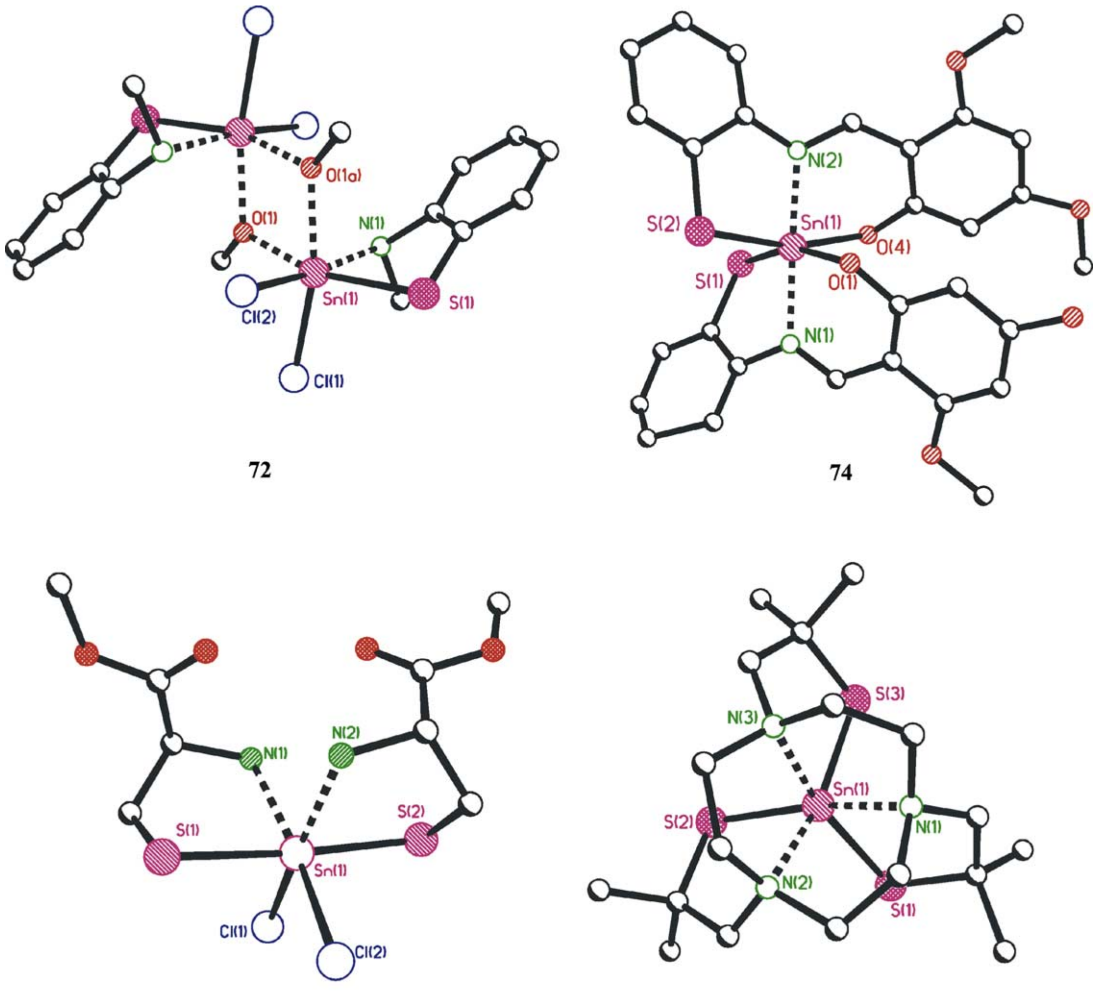

72 **74** **75** **77**

Fig. 13. Molecular structures of hexaco-ordinate group 14 complexes: All H atoms are omitted for clarity. Of the 2-methoxybenzyl substituent at the N atom in **72**, only the directly bound C atom is shown.

One of the applications of D-penicillamine, H_2L^{14}, in chelation therapy is the treatment of lead poisoning. The crystal structure of the corresponding complex, **76**, shows Pb^{II} in a strongly distorted ψ-pbp geometry. One of the O atoms of the carboxyl group is part of a five-membered chelating ring, and forms a shorter Pb–O bond than the other O atom, which co-ordinates to a neighboring Pb^{II}. The S atom acts in a μ^3 bridging mode, the Pb–S distance within the chelating

Table 12
Selected structural parameters describing the co-ordination mode in tetraco-ordinate Sn^{II}, and Pb^{II} complexes

Compound	CM(M)	*d*(M–S)	*d*(M–N)	*a*(S–M–S)	*d*(N–M–N)	τ[a]	References
$[Sn(L^{18b})Cr(CO)_5]$, **58**	$Pb(NS_2Cr)$	2.423(1)/2.426(1)	2.400(4)	104.9(1)	–	–	
$[Pb(L^{1a})_2]$, **59a**	$Pb(N_2S_2)$	2.633(3)/2.639(3)	2.550(8)/2.626(9)	99.2(1)	149.3(3)	0.835	[142]
$[Pb(L^{1a})_2\{PbCl(L^{1a})\}_2]$, **59b**	$Pb(N_2S_2)$	2.635(2)	2.592(6)	93.5(1)	149.9(2)	0.940	[142]
$[Sn(L^{2c})_2]$, **60**	$Sn(N_2S_2)$	2.520(1)/2.521(1)	2.412(4)/2.537(4)	100.2(1)	146.3(1)	0.768	[143]
$[Pb(L^{8a})_2]$, **61a**	$Pb(N_2S_2)$	2.715	2.481	99.1	137.2	0.535	[144]
$[Pb(L^{8d})_2]$, **61b**	$Pb(N_2S_2)$	2.617/2.639	2.591/2.691	93.1	139.9	0.780	[145]
$[Pb(L^{8f})_2]$, **61c**	$Pb(N_2S_2)$	2.617/2.653	2.569/2.604	93.9	143.6	0.829	[38]
$[Sn(L^{18b})]_2$, **62**	$Sn(NS_3)$	2.458(2)–2.615(2)[b]					
		2.709(2)–2.991(2)[c]	2.636(5)–2.971(6)	75.1(1)–97.5(1)	–	0.637–0.938	[146]

[a] For definition of structural parameter τ in pentaco-ordinate complexes, see Section 1. Here, τ is only given for Sn^{IV} complexes with tbp configuration but not for Pb^{II} complexes which exhibit ψ-octahedral geometry.

[b] M–S distances within chelating ring.

[c] M···S distances in M–S···M bridges.

Table 13
Selected structural parameters describing the co-ordination mode in pentaco-ordinate Sn^{IV}, and Pb^{II} complexes

Compound	CM(M)	*d*(M–S)	*d*(M–N)	*d*(M–X^1)	*d*(M–X^2)	τ[a]	References
[SnPh$_3$(L^{1a})], **63**	Sn(NSC$_3$)	2.426(2)	2.647(6)	2.132(7)–2.179(1)		0.845	[147]
[SnMe$_2$(L^{16a})], **64a**[b]	Sn(NSC$_2$O)	2.554(1)	2.176(4)	2.106(5)/2.125(6)	2.130(4)	0.562	[148]
[SnPh$_2$(L^{16c})], **64b**[b]	Sn(NSC$_2$O)	2.496(1)	2.217(3)	2.120(3)/2.126(3)	2.093(2)	0.518	[149]
[SnMe$_2$(L^{17})], **65a**[b]	Sn(NSC$_2$O)	2.528	2.148	2.101/2.111	2.184	0.529	[57]
[SnPh$_2$(L^{17})], **65b**[b]	Sn(NSC$_2$O)	2.502(1)	2.146(2)	2.127(3)/2.128(2)	2.165(2)	0.542	[150]
[SnEt$_2$Cl(L^{1c})], **66**[c]	Sn(NSC$_2$Cl)	2.414	2.388	2.132/2.156	2.544	0.623	[151]
[SnMe$_2$Cl(L^{2c})], **67**[c]	Sn(NSC$_2$Cl)	2.413(2)	2.43(1)	2.12(1)/2.16(1)	2.523(4)	0.773	[152]
[SnBzl$_2$Cl(L^{8a})], **68**[c]	Sn(NSC$_2$Cl)	2.386(2)	2.367(4)	2.133(6)/2.139(5)	2.475(5)	0.572	[153]
[SnMe$_2$(L^{18a})], **69a**	Sn(NS$_2$C$_2$)	2.428(2)/2.428(2)	2.566(6)	2.139(9)/2.159(9)	–	0.760	[154]
[CH$_2${SnPh(L^{18a})}$_2$], **69b**[d]	Sn(NS$_2$C$_2$)	2.409(2)–2.424(2)	2.651(7)–2.654(7)	2.129(8)–2.179(8)	–	0.610/0.755	[141]
[(Sn^{t}Bu$_2$)$_4$Ni(L^{28})], **70**[d]	Sn(NS$_2$C$_2$)	2.581(1)–2.595(1)	2.305(3)/2.318(3)	2.196(5)–2.204(5)	–	0.016/0.120	[155]
[Pb(L^{1e})(NO$_3$)], **71**	Pb(NS$_2$O$_2$)	2.645/2.792	2.606	2.689/2.983	–	–	[156]
[Pb(L^{1a})$_2${PbCl(L^{1a})}$_2$], **59b**	Pb(ClNS$_3$)	2.696(2)[e]	2.409(5)	2.791(2)	–	–	[142]
		3.036(2)/3.285(2)	–	–			

[a] For definition of structural parameter τ in pentaco-ordinate complexes see Introduction. Here, τ is only given for Sn^{IV} complexes with tbp configuration but not for Pb^{II} complexes which exhibit ψ-octahedral geometry.
[b] X^1 = C, X^2 = O.
[c] X^1 = C, X^2 = Cl.
[d] The two Sn atoms are crystallographically different.
[e] M–S distances within chelating ring.

Table 14
Selected structural parameters describing the co-ordination mode in hexaco-ordinate Sn^{IV}, and Pb^{II} complexes

Compound	CM(M)	*d*(M–S)	*d*(M–N)	*d*(M–X)	*a*(S–M–S)	*a*(N–M–N)	Reference
[SnCl$_2$(OMe)(L^{16b})$_2$]$_2$, **72**	Sn(NSO$_2$Cl$_2$)	2.431(1)	2.303(4)	2.086(2)/2.143(2)[a] 2.389(1)/2.393(1)[b]			[54]
[Sn(L^{15a})$_2$], **73**	Sn(N$_2$S$_2$O$_2$)	2.432(4)	2.19(1)	2.039(9)	180.0	180.0	[52]
[Sn(L^{16d})$_2$], **74**	Sn(N$_2$S$_2$O$_2$)	2.462(5)/2.484(5)	2.143(11)/2.154(11)	2.01(11)/2.067(10)	98.4(2)	171.7(5)	[56]
[SnCl$_2$(L^{2b})$_2$], **75**	Sn(N$_2$S$_2$Cl$_2$)	2.434(3)/2.446(3)	2.264(10)/2.309(10)	2.445(3)/2.445(3)	175.4(1)	85.0(4)	[157]
[Pb(L^{14})], **76**	Pb(NO$_2$S$_3$)	2.716–3.480	2.444	2.444/2.768		–	[158]
[Sn(L^{27b})]TcO$_4$·CHCl$_3$, **77**	Sn(N$_3$S$_3$), mer	2.411(3)–2.435(3)	2.292(8)–2.329(9)		101.2(1)–103.1(1)	76.0(3)–79.3(3)	[71]

[a] *d*(M–O).
[b] *d*(M–Cl).

Table 15
Complexes with tetra and pentaco-ordinate Bi^{III} atoms

Compound	CM(M)	*d*(M–S)	*d*(M–N)	*d*(M–X)	References
[Bi(L^{8a}){Mn(CO)$_2$(Cp′)}$_2$], **78**[a]	Bi(NSMn$_2$)	2.65(1)	2.54(2)	2.496(5)/2.504(4)	[159]
[Bi(L^{14})Cl], **79**	Bi(NSOCl)	2.527(2)	2.345(6)	2.414(5)/2.680(2)[b]	[160]
[Bi(L^{1a})$_2$]Cl, **80**	Bi(N$_2$S$_2$)	2.569(3)/2.608(3)	2.398(8)/2.528(9)		[161]
[Bi(L^{1c})$_2$Cl], **81**	Bi(N$_2$S$_2$Cl)	2.538(9)/2.572(9)	2.67(2)/2.84(2)	2.618(9)	[161]
[Bi(L^{8e})$_2$Cl], **82**	Bi(N$_2$S$_2$Cl)	2.532/2.590	2.628/2.880	2.579	[162]
[Bi(L^{1a})Cl$_2$]$_4$·HCl, **83**	Bi(NSCl$_3$)	2.530(7)	2.52(2)	2.548(8)–3.109(1)	[161]

[a] Cp′ = C$_5$H$_4$(CH$_3$).
[b] First value refers to *d*(Bi–O), second to *d*(Bi–Cl).

Table 16
Complexes with hexaco-ordinate Sb^{III} and Bi^{III} atoms

Compound	CM(M)	*d*(M–S)	*d*(M–N)	*a*(S–M–S)	*a*(N–M–N)	References
[Bi(L^{1a})$_2$(H$_2$O)(NO$_3$)], **84a**	Bi(N$_2$S$_2$O$_2$)	2.549(2)/2.589(2)	2.462(5)/2.455(6)	100.2(1)	143.7(1)	[163]
[Bi(L^{1a})$_2$(NO$_3$)], **84b**	Bi(N$_2$S$_2$O$_2$)	2.575(8)	2.48(2)	102.5	140.4	[161]
[Sb(L^{8b})$_3$], **85a**	Sb(N$_3$S$_3$)	2.488–2.527	2.656–2.780	83.6–87.5	109.4–115.3	[164]
[Sb(L^{8m})$_3$], **85b**	Sb(N$_3$S$_3$)	2.520–2.536	2.581–2.677	85.1–85.7	102.5–118.2	[44]
[Bi(L^{1a})$_3$], **86**	Bi(N$_3$S$_3$)	2.654(5)–2.748(7)	2.64(2)–2.83(2)	73.7–97.2	70.3–143.1	[161]
[Bi(L^{8a})$_3$], **87a**	Bi(N$_3$S$_3$)	2.591–2.673	2.686–2.845	73.5–92.5	76.2–150.1	[165]
[Bi(L^{8b})$_3$], **87b**	Bi(N$_3$S$_3$)	2.571–2.623	2.690–2.797	83.9–88.6	84.3–115.3	[166]

ring being much shorter than the other two Pb · · · S contacts (3.160 and 3.480 Å).

The ionic compound **77** (see Fig. 13) was formed in an attempt to prepare novel radiopharmaceuticals. The ligand forms a distorted octaheral co-ordination sphere with facial configuration around the Sn^{IV} centre, which is therefore shielded and does not co-ordinate to the pertechnetate (Tables 12–14).

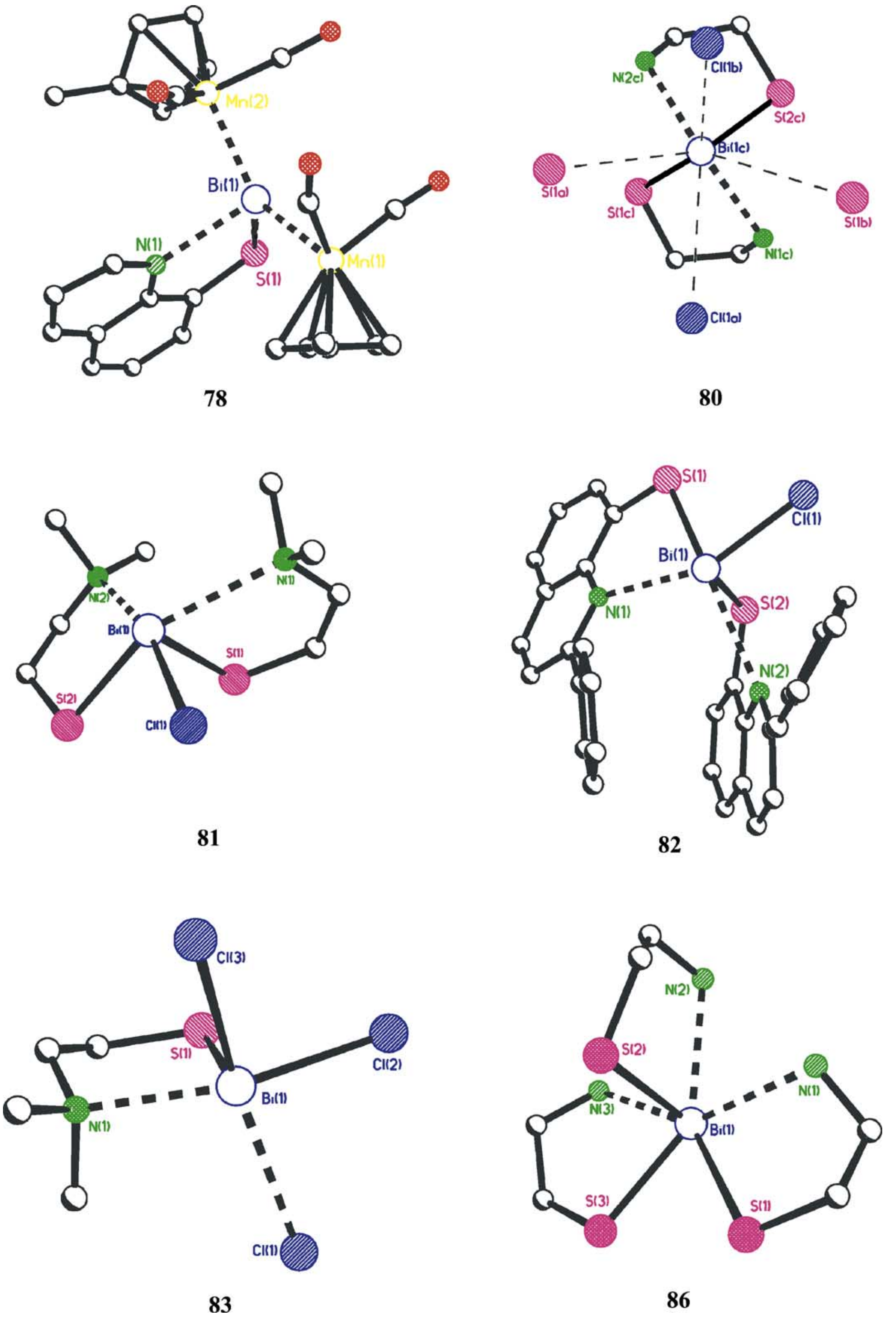

78 **80**

81 **82**

83 **86**

Fig. 14. Molecular structures of selected group 15 complexes. All H atoms are omitted for clarity. For **83** only one unit of the tetra-nuclear complex is shown.

3.5. *Group 15 complexes*

Sb and Bi are the only elements of group 15 with structurally known complexes with N,S-ligands, in which N···E interactions are present (E = group 15 element). No such complexes of pentavalent Sb or Bi are known, and in all cases but one, the central atom is trivalent. Hence, the lone pair at Sb or Bi may play a stereochemical role, thus increasing the structural variety.

3.5.1. *Complexes with tetra and pentaco-ordinate Bi^{III}*

78 (see Fig. 14) is an interesting compound, since a Bi^{I} atom is present, acting in a μ^2 bridging mode between two $Mn(CO)_2(Cp')$ units. The geometry at the Bi atom is between distorted tetrahedral and distorted ψ-tbp, as can be seen from the rather wide Mn–Bi–Mn angle (135.5(2)°) and the rather small N–Bi–S angle (74.7(8)°).

The mono-nuclear complex of **79** is ψ-tbp configured, with O and Cl in the apical positions. Anyhow, additional contacts are present in the solid state due to intermolecular interactions (d(Bi···O) = 2.698(5) and 2.779(5) Å, d(Bi···Cl) 3.182(2) Å), which lead to a (4 + 3) co-ordinate Bi atom with a distorted capped octahedral geometry. Similarly, **80** (see Fig. 14) exhibits a $Bi(N_2S_2)$ co-ordination mode in its first sphere, with the N atoms in the apical positions of a ψ-tbp configuration. A (4 + 4) co-ordinate Bi atom with a distorted square antiprismatic geometry results from two Bi···Cl (3.121 and 3.659 Å) and two Bi···S (3.479 and 3.720 Å) contacts in the solid state,.

Changing the N,S-ligand from L^{1a} to L^{1c} (**81**) or L^{8e} (**82**) has a dramatic impact on the co-ordination environment. In both cases (see Fig. 14), there are no intermolecular contacts of the Bi atom within the first co-ordination sphere, giving ψ-octahedrally configured Bi atoms.

There is π-interaction between the phenyl group of one ligand and the quinoline ring of the other in **82**, C···C and C···N distances being between 3.80 and 4.05 Å.

83 (see Fig. 14) is a tetra-nuclear complex, in which four $[Bi(L^{1a})Cl_2]$ units group surround one HCl molecule, the Cl atom of which co-ordinates to all four Bi atoms.

3.5.2. *Complexes with hexaco-ordinate Sb^{III} and Bi^{III}*

84a exhibits a strongly distorted octahedral structure, the N atoms being more or less *trans* to each other. The H_2O molecule and the NO_3^- ion both co-ordinate to the Bi^{III} atom, d(Bi–O) being 3.004(6) and 3.107(6) Å, respectively. The somewhat widened O–Bi–O angle of 111.6(2)° hints to a slight stereochemical activity of the lp in that region. The single complex molecule is associated with two of its neighbors via long Bi···S contacts (3.517(2) and 3.550(2) Å), forming chains of 6 + 2 co-ordinate Bi atoms in the solid state. A very similar co-ordination geometry occurs in **84b**, where NO_3^- acts as a bidentate ligand, d(Bi–O) being 3.05(2) Å.

85a and **85b** are the only Sb complexes known. Both exhibit *fac* $Sb(N_3S_3)$ octahedral configurations, i.e. the. Sb–S distances, a(S–Sb–S), a(N–Sb–N) and a(N–Sb–S) (154.7–157.9° and 155.9–156.5°, for **85a** and **85b**, respectively) are similar for both compounds. The Sb–N distances are much longer for **85a** which might be due to steric hindrance of the methyl group in 2-position of L^{8b}.

86 (see Fig. 14) and **87a** exhibit stereochemically active lone pairs at the Bi^{III} atom, with ψ-pbp configured $Bi(N_3S_3)$ co-ordination mode and the lp and one S atom in the apex positions. In the equatorial plane, the two S atoms are next to each other, $a(S^{eq}–Bi–S^{eq})$ being the most narrow of all S–Bi–S angles. As well the N atoms form two small and one large N–Bi–N angle, marking the contrast between a ψ-pbp and an octrahedral configuration.

In contrast Bi^{III} in **87b** does not display a stereochemically active lp, and hence possesses a distorted octahedral co-ordination geometry similar to **85a** and **85b**. It is *fac*-configured, with a(N–Sb–S) = 154.9–157.5° (Tables 15 and 16).

4. Summary and outlook

The complexes of the d^{10} metal ions with N,S ligands display a large variety of co-ordination geometries around the metal centers, with those of Zn^{2+} ions being the most well studied. Considering metal centers displaying at least one five-membered N,S-chelate ring, co-ordination numbers vary between four and eight. In the case of tetraco-ordinate complexes of $(n-1)\ d^{10}\ ns^0$ ions with $M(N_2S_2)$ co-ordination mode, the angle between MS_2 and MN_2 planes is a measure for the configuration. In all cases, distorted tetrahedral geometries were observed. A higher structural flexibility was observed for pentaco-ordinate complexes, where trigonal bipyramidal as well as square pyramidal configurations occur. The same applied for tetraco-ordinate $(n-1)\ d^{10}\ ns^2$ ions that display a stereochemically active lone pair in their complexes. In these cases, pseudo trigonal bipyramidal and pseudo square pyramidal configurations are known. The nuclearity of the thiolate complexes, i.e. mono- or oligo-/poly-nuclear depends on the number of co-ordinating atoms, D, per metal ion, M. Except for CuI, AgI and AuI, where a co-ordination number of two is observed in several cases, a D:M ratio of at least 4:1 seems to be necessary in order to obtain mono-nuclear complexes. Trends in d(M–S) and d(M–N) within a group reveal different acceptor strengths of M. In particular, for group 12 complexes, Zn–N interactions are stronger than Cd–N and Hg–N interactions, while in group 13, Al is a better acceptor than Ga or In.

The earlier structural investigations of the complexes treated in this paper mostly dealt with aspects of pure structural and co-ordination chemistry. In contrast, a lot of the more recent efforts were directed toward design of more sophisticated ligands with bio-mimetic properties in order to obtain metal co-ordination modes close to those found in vivo. Here, additionally to the structural investigations, kinetic and thermodynamic binding studies were performed and catalytic activities were studied in some cases.

Still, relatively little structural information is available for complexes of the naturally occurring ligands cysteamine, HL^{1a}, and cysteine, H_2La. Since these ligands are rather simple, their complexes are of fundamental interest to structural co-ordination chemistry. In that respect, reliable quantum chemical ab initio geometry optimizations, which were only reported in one case so far [142], would be feasible for small complexes and give additional insight. As well, structures of N,S-chelated metal ions bearing in vivo occurring anions like phosphate diesters, $[(RO)_2PO_2]^-$, or anions of amino acids, $[H_2NCH(R)COO]^-$, are not known. These complexes would be interesting models for metal mediated DNA–protein, RNA–protein or protein–protein binding. Finally, in contrast to the amount of structural data available for Zn^{II} complexes with N,S-ligands, relatively little is known about complexes of other two-valent ions like Cd^{II}, Hg^{II} or Pb^{II} with N,S-ligands. These complexes would provide useful information, since the latter ions are known to compete with Zn^{II} for protein binding sites [167–169].

References

[1] I.G. Dance, Polyhedron 5 (1986) 1037.
[2] B. Krebs, G. Henkel, Angew. Chem. Int. Ed. Engl. 30 (1991) 769.
[3] P.G. Blower, J.R. Dilworth, Coord. Chem. Rev. 76 (1987) 121.
[4] J.R. Dilworth, J. Hu, Adv. Inorg. Chem. 40 (1993) 411.
[5] M.A. Ali, S.E. Livingstone, Coord. Chem. Rev. 13 (1974) 101.
[6] S. Brooker, Coord. Chem. Rev. 222 (2001) 33.
[7] E.S. Raper, Coord. Chem. Rev. 61 (1985) 115.
[8] E.S. Raper, Coord. Chem. Rev. 153 (1996) 199.
[9] E.S. Raper, Coord. Chem. Rev. 165 (1997) 475.
[10] J.A. Garcia-Vazquez, J. Romero, A. Sousa, Coord. Chem. Rev. 193–195 (1999) 691.
[11] J.P. Danks, N.R. Champness, M. Schröder, Coord. Chem. Rev. 174 (1998) 417.
[12] J.R. Dilworth, N. Wheatley, Coord. Chem. Rev. 199 (2000) 89.
[13] J.S. Casas, M.S. Garcia-Tasende, J. Sordo, Coord. Chem. Rev. 209 (2000) 197.
[14] L. Pellerito, L. Nagy, Coord. Chem. Rev. 224 (2002) 111.
[15] S.B. Coghill, D. Hopwood, S.M. Pherson, S. Hislop, J. Pathol. 139 (1983) 105.
[16] T.C. Markello, I.M. Bernardini, W.A. Gahl, N. Engl. J. Med. 328 (1993) 1157.
[17] L.S. Goodman, A. Gilman, The Pharmacological Basis of Therapeutics, The Macmillan Company, New York, 1971, p. 945.
[18] G. Barone, R. Chaplin, T.G. Hibbert, A.T. Kana, M.F. Mahon, K.C. Molloy, I.D. Worsley, I.P. Parkin, L.S. Price, J. Chem. Soc., Dalton Trans. (2002) 1085.
[19] K. Osakada, T. Yamamoto, Inorg. Chem. 30 (1991) 2328.
[20] J. Cheon, D.S. Talaga, J.I. Zink, J. Am. Chem. Soc. 119 (1997) 163.
[21] D.D. Reynolds, M.K. Massad, D.L. Fields, D.J. Johnson, J. Org. Chem. 26 (1961) 5109.
[22] J. Harley-Mason, J. Chem. Soc. (1947) 320.
[23] D. Mastropaolo, J.A. Thich, J.A. Potenza, H.J. Schugar, J. Am. Chem. Soc. 99 (1977) 424.
[24] H.M. Woodburn, B.G. Pautler, J. Org. Chem. 19 (1954) 863.
[25] M. Friebe, A. Mahmood, H. Spies, R. Berger, B. Johannsen, A. Mohammed, M. Eisenhut, C. Bolzati, A. Davison, A.G. Jones, J. Med. Chem. 43 (2000) 2745.
[26] H. Albrich, H. Vahrenkamp, Chem. Ber. 127 (1994) 1223.
[27] R. Remuzon, D. Bouzard, P.D. Chesare, M. Essiz, J. Jaquet, A. Nicolau, Tetrahedron 51 (1995) 9657.
[28] P.S. Clezy, G.A. Smythe, Aust. J. Chem. 22 (1969) 239.
[29] D.-F. Shi, R.T. Wheelhouse, D. Sun, L.H. Hurley, J. Med. Chem. 44 (2001) 4509.
[30] U. Brand, H. Vahrenkamp, Chem. Ber. 128 (1995) 787.
[31] S. Ozturk, S. Ide, S.G. Oztas, N. Ancin, M. Tuzun, H.K. Fun, Z. Kristallogr. 214 (1999) 763.
[32] P.J. Palmer, R.B. Trigg, J.V. Warrington, J. Med. Chem. 14 (1971) 248.
[33] O.A. D'yachenko, S.M. Aldoshin, L.O. Atovmyan, Koord. Khim. (Russ.) (Coord. Chem.) 3 (1977) 1753.
[34] L.Y. Pech, V.S. Fundamenskii, O.G. Matyukhina, Y.K. Ozols, A.P. Sturis, Y.A. Bankovskii, Koord. Khim. (Russ.) (Coord. Chem.) 10 (1984) 1427.
[35] I.R. Berzinya, V.K. Bel'skii, A.P. Sturis, Y.A. Bankovskii, Latv. PSR Zinat. Akad. Vestis, Khim. Ser. (1984) 395.
[36] L.Y. Pech, A.P. Sturis, Y.K. Ozols, S.K. Apinitis, V.N. Purmal, Latv. PSR Zinat. Akad. Vestis, Khim. Ser. (1982) 271.
[37] I.R. Berzinya, O.G. Matyukhina, V.K. Bel'skii, Y.V. Ashaks, Y.A. Bankovskii, Latv. PSR Zinat. Akad. Vestis, Khim. Ser. (1985) 18.
[38] L. Pech, Y. Bankovsky, V. Fundamensky, A. Sturis, A. Bruvere, Latv. Khim. Z. (Latv. J. Chem.) (1992) 488.
[39] Y.A. Bankovskii, Y.E. Leeis, Latv. PSR Zinat. Akad. Vestis, Khim. Ser. (1971) 105.
[40] Y.A. Bankovsky, I.R. Berzinya, Y.V. Ashaks, I.A. Ephimenko, V.S. Fundamensky, Zh. Neorg. Khim. (Russ.) (Russ. J. Inorg. Chem.) 39 (1994) 603.
[41] A.D. Ozola, Y.K. Ozols, A.A. Kemme, M.F. Bundule, Y.Y. Bleidelis, Y.V. Ashaks, Y.A. Bankovskii, Zh. Strukt. Khim. (Russ.) (Russ. J. Struct. Chem.) 26 (1985) 107.
[42] A. Kawase, H. Freiser, Anal. Chem. 39 (1967) 22.
[43] O.G. Matyukhina, A.N. Sobolev, Y.E. Leeis, Y.K. Ozols, V.S. Fundamenskii, Y.A. Bankovskii, Koord. Khim. (Russ.) (Coord. Chem.) (1985) 264.
[44] I. Berzina, V. Belsky, Y. Bankovsky, J. Asaks, G. Jansons, Latv. Khim. Z. (Latv. J. Chem.) (1992) 477.
[45] M. Handa, M. Mikuriya, Z.J. Zhong, H. Okawa, S. Kida, Bull. Chem. Soc. Jpn. 61 (1988) 3883.
[46] R.P. Houser, V.G. Young, W.B. Tolman, J. Am. Chem. Soc. 118 (1996) 2101.
[47] U. Brand, H. Vahrenkamp, Inorg. Chim. Acta 308 (2000) 97.
[48] S.C. Chang, V.V. Karambelkar, R.C. di'Targiani, D.P. Goldberg, Inorg. Chem. 40 (2001) 194.
[49] J. Castro, J. Romero, J.A. Garcia-Vazquez, M.L. Duran, A. Castineiras, A. Sousa, D.E. Fenton, J. Chem. Soc., Dalton Trans. (1990) 3255.
[50] U. Brand, H. Vahrenkamp, Chem. Ber. 129 (1996) 435.
[51] C. Sudbrake, H. Vahrenkamp, Z. Anorg. Allg. Chem. 627 (2001) 857.
[52] E. Labisbal, J.A. Garcia-Vazquez, J. Romero, A. Sousa, A. Castineiras, C. Maichle-Mossmer, U. Russo, Inorg. Chim. Acta 223 (1994) 87.
[53] R.G. Charles, H. Freiser, J. Org. Chem. 18 (1953) 422.
[54] S.-B. Teo, S.-G. Teoh, R.C. Okechukwu, H.-K. Fun, Polyhedron 13 (1994) 2223.
[55] E. Labisbal, J.A. Garcia-Vazquez, C. Gomez, A. Macias, J. Romero, A. Sousa, U. Englert, D.E. Fenton, Inorg. Chim. Acta 203 (1993) 67.
[56] E. Labisbal, A.D. Blas, J.A. Garcia-Vazquez, J. Romero, M.L. Duran, A. Sousa, N.A. Bailey, D.E. Fenton, P.B. Leeson, Polyhedron 11 (1992) 227.
[57] S.-B. Teo, S.-G. Teoh, R.C. Okechukwu, C. Wei, J. Coord. Chem. 28 (1993) 81.
[58] U. Brand, H. Vahrenkamp, Z. Anorg. Allg. Chem. 622 (1996) 213.

[59] H. Kurosaki, T. Tawada, S. Kawasoe, Y. Ohashi, M. Goto, Bioorg. Med. Chem. Lett. 10 (2000) 1333.
[60] J.M. Jeong, Y.S. Lee, Y.L. Kim, D.S. Lee, J.K. Chung, J.H. Cho, Y.G. Suh, M.C. Lee, J. Labelled Compd. Radiopharm. 44 (2001) 605.
[61] W.J. Hu, D. Barton, S.J. Lippard, J. Am. Chem. Soc. 95 (1973) 1170.
[62] A. Corbin, K.F. Miller, N. Pariyadath, S. Wherland, A.E. Bruce, E.I. Stiefel, Inorg. Chim. Acta 28 (1984) 1853.
[63] J. Schneider, M. Köckerling, R. Kopitzky, G. Henkel, Eur. J. Inorg. Chem. (2003) 1727.
[64] H.F. Kung, C.C. Yu, J. Billings, M. Molnar, M. Blau, J. Med. Chem. 28 (1985) 1280.
[65] L.C. Francesconi, B.-L. Liu, J.J. Billings, P.J. Carroll, G. Graczyk, H.F. Kung, Chem. Commun. (1991) 94.
[66] U. Brand, R. Burth, H. Vahrenkamp, Inorg. Chem. 35 (1996) 1083.
[67] L.F. Lindoy, V.L. Goedken, D.H. Busch, Chem. Commun. (1972) 683.
[68] C. Sudbrake, H. Vahrenkamp, Eur. J. Inorg. Chem. (2001) 751.
[69] Y. Li, A.E. Martell, R.D. Hancock, J.H. Reibenspies, C.J. Anderson, M.J. Welch, Inorg. Chem. 35 (1996) 404.
[70] D.A. Moore, P.E. Fanwick, M.J. Welch, Inorg. Chem. 29 (1990) 672.
[71] C.S. John, C.E. Costello, E.O. Schlemper, Polyhedron 11 (1992) 2651.
[72] C.S. Velazquez, E. Broderick, M. Sabat, A.G.M. Barrett, B.M. Hoffman, J. Am. Chem. Soc. 112 (1990) 7408.
[73] I. Casals, P. Gonzalez-Duarte, C. Lopez, X. Solans, Polyhedron 9 (1990) 763.
[74] D.M. Knotter, H.L.v. Maanen, D.M. Grove, A.L. Spek, G.v. Koten, Inorg. Chem. 30 (1991).
[75] D.M. Knotter, M.D. Jansen, D.M. Grove, W.J.J. Smeets, E. Horn, A.L. Spek, G.v. Koten, Inorg. Chem. 30 (1991) 4361.
[76] S. Kitagawa, M. Munakata, H. Shimono, S. Matsuyama, H. Masuda, J. Chem. Soc., Dalton Trans. (1990) 2105.
[77] M.D. Janssen, J.G. Donkervoort, S.B.v. Berlekom, A.L. Spek, D.M. Grove, G.v. Koten, Inorg. Chem. 35 (1996) 4752.
[78] P. Pyykkö, Chem. Rev. 97 (1997) 597.
[79] D. Habibi, E. Ghaemi, R.V. Parish, R.G. Pritchard, Polyhedron 18 (1999) 2977.
[80] L.G. Kuz'mina, J.A.K. Howard, K.I. Grandbegr, E.G. Il'ina, A.V. Churakov, personal communication, 2003.
[81] R.H. Prince, in: G. Wilkinson, R. Gillard, D. McCleverty (Eds.), Comprehensive Coordination Chemistry, Pergamon Press, Oxford, UK, 1987, p. 925.
[82] B.L. Vallee, D.S. Auld, Acc. Chem. Res. 26 (1993) 543.
[83] H. Eklund, B. Nordström, E. Zeppezauer, G. Soderlund, I. Ohlsson, T. Bowie, B.O. Soderberg, O. Tapia, C.I. Bränden, J. Mol. Biol. 102 (1976) 27.
[84] M.H. Bracey, J. Christiansen, P. Tovar, S.P. Cramer, S.G. Bartlett, Biochemistry 33 (1994) 13126.
[85] A.J. Dent, D. Beyersmann, C. Block, S.S. Hasnain, Biochemistry 29 (1990) 7822.
[86] U. Brand, H. Vahrenkamp, Inorg. Chem. 34 (1995) 3285.
[87] D. Mastropaolo, J.A. Thich, J.A. Potenza, H.J. Schugar, J. Am. Chem. Soc. 99 (1977) 424.
[88] B. Cohen, D. Mastropaolo, J.A. Potenza, H.J. Schugar, Acta Crystallogr., Sect. B: Struct. Crystallogr. Cryst. Chem. 34 (1978) 2859.
[89] P. Bell, W.S. Sheldrick, Z. Naturforsch. 39B (1984) 1732.
[90] R. Burth, H. Vahrenkamp, Inorg. Chim. Acta 282 (1998) 193.
[91] L.Y. Pech, O.G. Matyukhina, A.N. Sobolev, K. Sturis, A.P. Sturis, Y.A. Bankovskii, Y.K. Ozols, Koord. Khim. (Russ.) (Coord. Chem.) 12 (1986) 549.
[92] T. Kawamoto, Y. Kushi, J. Chem. Soc., Dalton Trans. (1992) 3137.
[93] I.R. Berzinya, V.K. Bel'skii, A.K. Sturis, Y.V. Ashaks, Y.A. Bankovskii, L.Y. Pech, Latv. PSR Zinat. Akad. Vestis, Khim. Ser. (1987) 42.
[94] L. Pech, A. Sobolev, Y. Bankovsky, A. Sturis, G. Jankevics, Latv. PSR Zinat. Akad. Vestis, Khim. Ser. (1989) 547.
[95] O.G. Matyukhina, Y.K. Ozols, B.T. Ibragimov, Y.E. Leeis, L.E. Terent'eva, N.V. Belov, Zh. Strukt. Khim. (Russ.) (Russ. J. Struct. Chem.) 22 (1981) 144.
[96] M.N. Potenza, R.T. Stibrany, J.A. Potenza, H.J. Schugar, Acta Crystallogr., Sect. C: Cryst. Struct. Commun. 48 (1992) 545.
[97] T. Konno, Y. Yonenobu, J. Hidaka, K. Okamoto, Inorg. Chem. 33 (1994) 861.
[98] Y. Miyashita, N. Sakagami, Y. Yamada, T. Konno, J. Hikada, K. Okamoto, Bull. Chem. Soc. Jpn. 71 (1998) 661.
[99] Y. Yamada, K. Okamoto, Chem. Lett. (1999) 315.
[100] K. Okamoto, C. Sasaki, Y. Yamada, T. Konno, Bull. Chem. Soc. Jpn. 72 (1999) 1685.
[101] Y. Yamada, Y. Miyashita, K. Fujisawa, K. Okamoto, Bull. Chem. Soc. Jpn. 74 (2001) 97.
[102] M. Mikuriya, X. Jian, S. Ikemi, T. Kawahashi, H. Tsutsumi, Bull. Chem. Soc. Jpn. 71 (1998) 2161.
[103] A. Becker, I. Schlichting, W. Kabsch, D. Groche, S. Schultz, A.F.V. Wagner, Nat. Struct. Biol. 5 (1998) 1053.
[104] S. Chang, R.D. Sommer, A.L. Rheingold, D.P. Goldberg, Chem. Commun. (2001) 2396.
[105] G.J. Kleywegt, W.G.R. Wiesmeijer, G.J.V. Driel, W.L. Driessen, J. Reedijk, J.H. Noordik, J. Chem. Soc., Dalton Trans. (1985) 2177.
[106] D.J.E. Spencer, A.J. Blake, S. Parsons, M. Schröder, J. Chem. Soc., Dalton Trans. (1999) 1041.
[107] A.W. Addison, T.N. Rao, J. Reedijk, R. Rijn, G.C. Verschoor, J. Chem. Soc., Dalton Trans. (1984) 1349.
[108] D.C. Liles, M. McPartlin, P.A. Tasker, J. Am. Chem. Soc. 99 (1977) 7704.
[109] M. Ruf, R. Burth, K. Weis, H. Vahrenkamp, Chem. Ber. 129 (1996) 1251.
[110] S.C. Shoner, K.J. Humphreys, D. Barnhart, J.A. Kovacs, Inorg. Chem. 34 (1995) 5933.
[111] V.L. Goedken, G.G. Christoph, Inorg. Chem. 12 (1973) 2316.
[112] T. Tuntulani, J.H. Reibenspies, P.J. Farmer, M.Y. Darensbourg, Inorg. Chem. 31 (1992) 3497.
[113] L.G. Kuz'mina, Y.T. Struchkov, E.M. Rokhlina, D.N. Kravtsov, Zh. Strukt. Khim. (Russ.) (Russ. J. Struct. Chem.) 24 (1983) 130.
[114] I. Casals, P. Gonzalez-Duarte, W. Clegg, C. Foces-Foces, F.H. Cano, M. Martinez-Ripoll, M. Gomez, X. Solans, J. Chem. Soc., Dalton Trans. (1991) 2511.
[115] C. Brückner, S.J. Rettig, D. Dolphin, Inorg. Chem. 39 (2000) 6100.
[116] L.Y. Pech, Y.K. Ozols, A.A. Kemme, Y.Y. Bleidelis, A.P. Sturis, Latv. PSR Zinat. Akad. Vestis, Khim. Ser. (1979) 259.
[117] L. Pech, Y. Bankovsky, I. Berzina, V. Bel'sky, A. Sobolev, J. Ashaks, Latv. Khim. Z. (Latv. J. Chem.) (1997) 87.
[118] O.G. Matyukhina, A.N. Sobolev, I.R. Berzinya, Y.V. Ashaks, Y.A. Bankovskii, Koord. Khim. (Russ.) (Coord. Chem.) 11 (1985) 822.
[119] O.G. Matyukhina, Y.K. Ozols, A.N. Sobolev, Y.E. Leeis, Y.A. Bankovskii, Latv. PSR Zinat. Akad. Vestis, Khim. Ser. (1983) 672.
[120] I.R. Berzinya, V.K. Bel'skii, Y.K. Ozols, A.P. Sturis, Latv. PSR Zinat. Akad. Vestis, Khim. Ser. (1984) 52.
[121] O.G. Matyukhina, A.N. Sobolev, L.Y. Pech, Y.E. Leeis, Y.K. Ozols, Y.A. Bankovskii, Zh. Strukt. Khim. (Russ.) (Russ. J. Struct. Chem.) 26 (1985) 113.
[122] E. Dubler, E. Gyr, Inorg. Chem. 27 (1988) 1466.
[123] E. Labisbal, J. Romero, J.A. Garcia-Vazquez, C. Gomez, A. Sousa, R. Pritchard, C.A. McAuliffe, Polyhedron 13 (1994) 1735.
[124] H.C. Freeman, F. Huq, G.N. Stevens, Chem. Commun. (1976) 90.
[125] T.G. Fawcett, C.C. Ou, J.A. Potenza, H.J. Schugar, J. Am. Chem. Soc. 100 (1978) 2058.
[126] M. Mikuriya, X. Jian, S. Ikemi, T. Kawahashi, H. Tsutsumi, A. Nakasone, J.-W. Lim, Inorg. Chim. Acta 312 (2001) 183.
[127] J.A. Francis, S.G. Bott, A.R. Barron, Polyhedron 18 (1999) 2211.

[128] H.F. Kung, B.-L. Liu, D. Mankoff, M.-P. Kung, J.J. Billings, L.C. Francesconi, A. Alavi, J. Nucl. Med. 31 (1990) 1635.

[129] M.J. Taylor, Compr. Coord. Chem. 3 (1987) 105.

[130] D.G. Tuck, Compr. Coord. Chem. 3 (1987) 153.

[131] C.N. McMahon, J.A. Francis, S.G. Bott, A.R. Barron, J. Chem. Soc., Dalton Trans. (1999) 67.

[132] C. Jones, F.C. Lee, G.A. Koutsantonis, M.G. Gardiner, C.L. Raston, J. Chem. Soc., Dalton Trans. (1996) 829.

[133] A.N. Chekhlov, Zh. Strukt. Khim. (Russ.) (Russ. J. Struct. Chem.) 35 (1994) 178.

[134] Y.Y. Zheng, S. Saluja, G.P.A. Yap, M. Blumenstein, A.L. Rheingold, K.C. Francesconi, Inorg. Chem. 35 (1996) 6656.

[135] I.R. Berzina, O.G. Matyukhina, A.N. Sobolev, Y.V. Ashaks, Y.A. Bankovskii, V.S. Fundamenskii, Latv. PSR Zinat. Akad. Vestis, Khim. Ser. (1985) 25.

[136] L. Pech, Y. Bankovsky, V. Bel'sky, E. Silina, J. Ashaks, A. Sturis, Latv. Khim. Z. (Latv. J. Chem.) (2000) 3.

[137] L.Y. Pech, V.S. Fundamenskii, Y.A. Bankovskii, I.R. Berzinya, A.P. Sturis, V.N. Purmal, Latv. PSR Zinat. Akad. Vestis, Khim. Ser. (1986) 414.

[138] L. Pech, Y. Bankovsky, A. Kemme, V. Belsky, E. Silina, Y. Ashaks, Khim. Get. Soedin., SSSR (Russ.) (Chem. Hetero. Compnd.) (2002) 789.

[139] U. Bossek, D. Hanke, K. Wieghardt, Polyhedron 12 (1993) 1.

[140] R. Ma, M.J. Welch, J. Reibenspies, A.E. Martell, Inorg. Chim. Acta 236 (1995) 75.

[141] R. Willem, M. Gielen, J. Meunier-Piret, M.v. Meerssche, K. Jurkschat, A. Tzschach, J. Organomet. Chem. 277 (1984) 335.

[142] H. Fleischer, D. Schollmeyer, Inorg. Chem. 43 (2004) 5529.

[143] J.E. Anderson, S.M. Sawtelle, J.S. Thompson, S.A.K. Nguyen, J. Calabrese, Inorg. Chem. 31 (1992) 2778.

[144] V.M. Agre, E.A. Shugam, Zh. Strukt. Khim. (Russ.) (Russ. J. Struct. Chem.) 12 (1971) 102.

[145] L.Y. Pech, V.S. Fundamenskii, Y.K. Ozols, A.B. Sturis, V.N. Parmal, Y.A. Bankovskii, Latv. PSR Zinat. Akad. Vestis, Khim. Ser. (1985) 394.

[146] K. Jurkschat, M. Scheer, A. Tzschach, J. Meunier-Piret, M.V. Meerssche, J. Organomet. Chem. 281 (1984) 173.

[147] B.D. James, R.J. Magee, W.C. Patalinghug, B.W. Skelton, A.H. White, J. Organomet. Chem. 467 (1994) 51.

[148] G.-Y. Yeap, H.-K. Fun, S.-B. Teo, S.-G. Teoh, Acta Crystallogr., Sect. C: Cryst. Struct. Commun. 48 (1992) 1109.

[149] H. Preut, H.-J. Haupt, F. Huber, R. Cefalu, R. Barbieri, Z. Anorg. Allg. Chem. 407 (1974) 257.

[150] R.C. Okechukwu, H.-K. Fun, S.-G. Teoh, S.-B. Teo, K. Chinnakali, Acta Crystallogr., Sect. C: Cryst. Struct. Commun. 49 (1993) 368.

[151] D. Couce, G. Valle, U. Casellato, R. Graziani, U. Russo, Z. Kristallogr.: New Cryst. Struct. 215 (2000) 285.

[152] G. Domazetis, M.F. Mackay, R.J. Magee, B.D. James, Inorg. Chim. Acta 34 (1979) L247.

[153] E. Kellö, V. Vrabel, A. Lycka, J. Sivy, Acta Crystallogr., Sect. C: Cryst. Struct. Commun. 49 (1993) 1943.

[154] M. Dräger, J. Organomet. Chem. 251 (1983) 209.

[155] C.S. Velazquez, G.A. Fox, W.E. Broderick, K.A. Andersen, O.P. Anderson, A.G.M. Barrett, B.M. Hoffman, J. Am. Chem. Soc. 114 (1992) 7416.

[156] I.G. Dance, P.J. Guerney, Aust. J. Chem. 34 (1981) 57.

[157] S. Calogero, G. Valle, P.A. Cusack, P.J. Smith, J.D. Donaldson, Inorg. Chim. Acta 67 (1982) 95.

[158] H.C. Freeman, G.N. Stevens, I.F.T. Junior, Chem. Commun. (1974) 366.

[159] S.J. Davies, N.A. Compton, G. Huttner, L. Zsolnai, S.E. Garner, Chem. Ber. 124 (1991) 2731.

[160] W.A. Herrmann, E. Herdtweck, L. Pajdla, Chem. Ber. 126 (1993) 895.

[161] G.G. Briand, N. Burford, T.S. Cameron, W. Kwiatkowski, J. Am. Chem. Soc. 120 (1998) 11374.

[162] I.R. Berzinya, O.G. Matyukhina, V.K. Bel'skii, Y.V. Ashaks, Y.A. Bankovskii, Latv. PSR Zinat. Akad. Vestis, Khim. Ser. (1985) 161.

[163] W.A. Herrmann, P. Kiprof, W. Scherer, L. Pajdla, Chem. Ber. 125 (1992) 2657.

[164] E.Y. Silin', Y.A. Bankovsky, V.K. Bel'sky, A.I. Stash, Y.V. Ashaks, Latv. Khim. Z. (Latv. J. Chem.) (1997) 24.

[165] E. Silina, Y.A. Bankovskii, V.K. Bel'sky, A.I. Stash, L.Y. Pech, Y.V. Ashaks, Zh. Neorg. Khim. (Russ.) (Russ. J. Inorg. Chem.) 45 (2000) 1150.

[166] E. Silina, Y. Bankovsky, V. Belsky, A. Stass, J. Asaks, Latv. Khim. Z. (Latv. J. Chem.) (1996) 57.

[167] T. Dudev, C. Lim, Chem. Rev. 103 (2003) 773.

[168] J.C. Payne, M.A.t. Horst, H.A. Godwin, J. Am. Chem. Soc. 121 (1999) 6850.

[169] B.A. Krizek, D.L. Merkle, J.L. Berg, Inorg. Chem. 32 (1993) 937.